UNIVERSITY OF CALIFORNIA
SANTA CRUZ

TOPICS IN COSMOLOGY AND DARK MATTER

A dissertation submitted in partial satisfaction of the
requirements for the degree of

DOCTOR OF PHILOSOPHY

in

PHYSICS

by

Yan Yu

June 2023

The Dissertation of Yan Yu
is approved:

Professor Michael Dine, Chair

Professor Stefano Profumo

Professor Anthony Aguirre

Peter Biehl
Vice Provost and Dean of Graduate Studies

Table of Contents

List of Figures

List of Tables

Abstract

Topics in Cosmology and Dark Matter

by

Yan Yu

We study the obstacles to constructing metastable de Sitter space in string theory. We explain that it is very difficult to find stationary points for which both the string coupling is small and compactification radii are large even allowing the possibility of arbitrarily large fluxes, and a set of small perturbations of any would-be metastable de Sitter state, classically, will evolve to uncontrollable singularities. We study the Trans-planckian Censorship Conjecture and show a conflict between the TCC and conventional conjectures about the string landscape. We calculate, as a function of the primordial black holes mass and initial abundance, the combination of dark matter particle masses and number of effective dark degrees of freedom leading to the right abundance of dark matter today, whether or not evaporation stops around the Planck scale.

Acknowledgments

I am profoundly grateful to my advisors, Michael Dine and Stefano Profumo, for patiently teaching me understand physics, sharing ideas with me and encouraging me. I am indebted to Anthony Aguirre, Howard Haber, Onuttom Narayan, Sriram Shastry for their meticulous teaching.

I am also grateful to Logan Morrison, Shijun Sun, Duncan Wood and Jamie Law-Smith for their collaborations and discussions during our projects.

It is my fortune throughout the years to share the friendship with amazing fellows in both Astro and Phys department: Enia Xhakaj, Felipe Ardila, Zack Briesemeister, César Rojas Bravo, Brittany Miles , Jiani Ding, Yifei Luo, Yao Tang, Yuting Feng, Siyu Zhu, Yuzhan Zhao, Kejun Li, Nick Hamer, Joseph Connell, Evan Frangipane, Nolan Smyth.

I would also like to thank my friends outside physics, Zimu, Zavier, Lofty, Hongzhan, Hang, Jiaming, Erdong, who make my life beyond academic colorful and entertaining.

Finally, I thank my family for their support and encouragement.

The text of this dissertation includes material from the previously published papers:

Michael Dine, Jamie AP Law-Smith, Shijun Sun, Duncan Wood, and Yan Yu. "Obstacles to con- structing de Sitter space in string theory." Journal of High Energy Physics 2021, no. 2 (2021): 1-19.

Logan Morrison, Stefano Profumo and Yan Yu. "Melanopogenesis: dark matter of (almost) any mass and baryonic matter from the evaporation of primordial black holes weighing a ton (or less)". Journal of Cosmology and Astroparticle Physics 2019.05 (2019): 005.

Michael Dine, and Yan Yu. "Comments on the Transplanckian Censorship Conjecture." Journal of High Energy Physics 2023.5 (2023): 1-11.

Part I

de Sitter Space in String Theory

Chapter 1

Introduction

Measurements of mass density Ω_M, and cosmological-constant energy density Ω_Λ from supernovae [1], CMB [2], and Large Scale Structure observations [3] showed observational evidence of accelerating universe with a positive cosmological constant. Cosmological constant is about

$$\lambda = 10^{-47}\mathrm{GeV}^4$$

However, natural value might be said to be M_p^4 because we could estimate the vacuum energy density by summing the zero-point energies in momentum space with some mass m up to a cutoff $\Lambda \approx (8\pi G)^{-1/2}$,

$$\langle\rho\rangle = \int_0^\Lambda \frac{4\pi k^2 dk}{(2\pi)^3}\frac{1}{2}\sqrt{k^2+m^2} \approx \frac{\Lambda^4}{16\pi^2} = 2\times 10^{71}\mathrm{GeV}^4 \tag{1.1}$$

This is about 120 orders of magnitude larger than the observed cosmological constant. In Weinberg's paper, he introduced a different approach to cosmological constant which is named anthropic principle [4]. Basically it says the cosmological constant

has to be that number in order to let intelligent life arise. The cosmological constant should not be too large, otherwise the universe would very early enter an eternal exponentially expanding de Sitter phase, which would make the gravitational condensation weak and prevent the growth of structure, and thus observers would be hard to develop without the formation of galaxies and stars. Thus the anthropic principle take accounts the smallness of cosmological constant. We should notice that this idea presupposes a large possible set of vacuum states of the underlying theory, with some distribution of properties, which we called the cosmic landscape. Next, we will introduce the landscape in string theory.

In the modern language of string theory, instead of different theories, we have different solutions of a master theory. By varying the dynamical moduli, which usually refers to the size and shape parameters of the compact internal space that 4-dimensional string theory needs, we are able to move around the solution space of supersymmetric vacua. In low energy approximation the moduli appear as massless scalar fields, and the solutions of the theory are characterized by the values of the scalar field moduli. Changing the value of such scalar involves a change of potential energy, and the local minima of the potential are the vacua. If the local minimum is an absolute minimum the vacuum is stable, otherwise it is metastable. The value of the potential energy at the minimum is the cosmological constant for that vacuum, and for a positive cosmological constant, the vacuum is de Sitter space.

However, the continuum of solutions in the supersymmetric moduli space are all with vanishing cosmological constant, and we have to believe that there are other

separate islands beside the supersymmetric moduli space. The fact that the cosmological constant is small and positive requires the vacua include states with non–zero vacuum energy. Also the vacuum energy and the term of $\lambda/8\pi G$ must cancel to about 120 decimal places, thus the fine tuning of the cosmological constant makes it hard to find a vacuum in the observed range unless there are an enormous number of solutions with almost every possible value of λ, and we call the space of all such string theory vacua the landscape.

The supersymmetric moduli space of string theory is a special part of the landscape where the potential is zero or negative, and these vacua are marginally stable. Now since evidence of observation indicates positive c.c, corresponding to positive vacuum energy and de Sitter solution, the question becomes: does de Sitter Space live in the landscape of string theory? Some *models* were provided by Bousso and Polchinski [5], and subsequently by Kachru, Kallosh, Linde and Trevedi [6], in which they subtly used ingredients of string theory including fluxes, branes, anti–branes and instantons to construct a solution with a small positive cosmological constant. But these models are not reliable, they are not based on any systematic approximation. Unfortunately, de Sitter space has troubles in string theory. The only objects in string theory which are rigorously defined are S–Matrix elements, which require the existence of an asymptotic boundary in string theory. However, de Sitter space does not allow this kind of asymptotic description. The space-time asymptotic boundaries of de Sitter space are problematic, and there are no known observables in de Sitter Space which can substitute for S–matrix elements. The problem of defining S-matrix elements in de Sitter

space is that the de Sitter vacua of string theory are metastable. According to Dine and Seiberg[7] there are always runaway solutions in string theory where the effective potential has a de Sitter vacuum at some $\Phi = \Phi_0$, but the absolute minimum occurs at $\Phi = \infty$ with exactly zero vacuum energy, and so it is always possible for de Sitter vacuum to decay onto the supersymmetric moduli space.

Given the fact that it is difficult to construct a de Sitter vacuum in string theory in a controlled approximation, Ooguri and Vafa suggests the possibility that meta-stable de Sitter space does not belong to the landscape [8], instead dS lies in what they call the swampland of string theory or a set of states which do not exist in string theory. In their conjecture the cosmological constant in our universe is positive but the scalar field is not at a minimum, as in quintessence models. Their criterion of the swampland is in the form of $|\Delta V| \geq c \cdot V$, where c is a positive constant, and this lower bound of $|\Delta V|$ forbids the de Sitter vacua. This would bring some possible implications for inflation, the nature of the currently observed dark energy, and implementing the anthropic explanation of the c.c. However, We will not address the conjecture in its full generality, but we will examine back to the starting point. The authors of [8] begin with the observation that it has proven difficult to construct de Sitter space in string theory. While there are constructions that appear to achieve a positive cosmological stationary point in a suitable effective action [9, 10], it is not clear that they are in any sense generic.

But one should first ask: what would it mean to construct de Sitter space in string theory? In most constructions, one starts with some classical solution of the

equations of critical string theory. These solutions invariably have moduli or pseudo-moduli. Then one adds features, such as fluxes, branes, and orientifold planes which give rise to a potential for these moduli, and looks for a local minimum with positive four-dimensional c.c. These attempts to construct de Sitter space generally raise two questions. First, what is the approximation scheme that might justify any such construction? Second, any would-be de Sitter space found in this way is necessarily, at best, metastable: inevitably there is a lower energy density in asymptotic regions of the original moduli space. Quantum mechanically, the purported de Sitter state cannot be eternal. It has a history; it will decay in the future and must have been created by some mechanism in the past. The quantum mechanics of this process is challenging to pin down. In this thesis, we will see that already classically, the notion of an eternal de Sitter space in string theory is problematic; small perturbations near the de Sitter stationary point of the effective action evolve to singular cosmologies.

In more detail, there are at least two challenges to any search for metastable de Sitter space in string theory:

1. One requires a small parameter(s) allowing a controlled approximation to finding stationary points of an effective action. Here one runs into the problem described in [7]. Without introducing additional, fixed parameters (i.e., introducing parameters not determined by moduli), would-be stationary points in the potential for the moduli lie at strong coupling. Typically, attacks on this problem (and the question of de Sitter space) exploit large fluxes. If there is to be a systematic approximation, it is necessary that the string coupling be small and compactifica-

tion radii large at any would-be stationary point found in this way. If the strategy is to obtain inverse couplings and radii scaled by some power of fluxes, it is also important that these fluxes (and possibly other discrete parameters) can be taken arbitrarily large, without spoiling the effective action treatment. Even allowing uncritically for this latter possibility, we will see that it is quite challenging to realize arbitrarily weak string coupling and large radius, with positive or *negative* c.c.[1]

2. If one finds such a stationary point, one must ask about stability. More precisely, in string theory, we are used to searching for suitable background geometries and field configurations by requiring that the evolution of excitations about these configurations is described by a unitary S matrix. Classically, at least in a flat background, this is the statement that any initial perturbation of the system has a sensible evolution to some final perturbation. Again, we will see that this requirement is problematic for any would-be classical de Sitter stationary point in such a theory; even if all eigenvalues of the mass-squared matrix (small fluctuation operator) are positive, large classes of small perturbations evolve to singular geometries.

The problem of evolution of small perturbations is connected with the properties of the moduli of string compactifications, described above. We consider, in particular, disturbances of the moduli fields in a classical, eternal de Sitter space. We will

[1]This point has been noted earlier [11–13]. A broad critique, applicable to many non-perturbative scenarios, has been put forward in [14].

see in this thesis that some small fluctuations in the far past are amplified, rolling over the barrier to a contracting universe that culminates in a big crunch singularity. As a result, already classically, there is no notion of an S matrix (in the sense of describing the future of any small disturbance of the system), even restricted to very small perturbations localized near the metastable minimum of the potential. Within our current collection of calculational tools, we lack any framework in string theory to study such singularities. As a result, we will explain, the problem of constructing de Sitter space in string theory is not, at least at present, accessible to systematic analysis.

Overall, then, we will argue that we lack theoretical methods to address, in any systematic fashion, the problem of constructing de Sitter space in string theory, much as we lack the tools to understand big bang or big crunch singularities in any controlled approximation. The existence of metastable de Sitter states may be plausible or not, but it is a matter of speculation.[2] The failure to find such states in any controlled analysis appears, at least at present, inevitable.

[2]Reference [15] gives non-perturbative arguments for the absence of de Sitter vacua in controlled approximations. Various scenarios for how de Sitter might arise, and how this might be understood, even lacking a systematic approximation, have been put forward. Among many examples, [16, 17] argue for a more refined version, based on explicit constructions; [18, 19] consider F-theory compactifications and associated prospects. [20] proposes another way in which de Sitter might arise. [21] takes a phenomenological view of the problem. An alternative discussion of de Sitter space in flux vacua appears in [14], who argues against flux stabilization on rather general grounds. [22] takes an optimistic view of the prospects for such constructions and [23–25] put forth several scenarios.

Chapter 2

Review of de Sitter Space

For a long time there's data from the Cosmic Microwave Radiation Background showing that the universe is extremely homogenous and isotropic, which implies that the spacetime of the universe is maximally symmetric. De Sitter space is the maximally symmetric spacetime with positive Ricci curvature, corresponding to positive cosmological constant. Here we will use two approaches to find the metric of de Sitter spacetime.

2.1 embedding a 4D hyperboloid in 5D Minkowski space

D-dimensional de Sitter spacetime can be viewed as a timelike hyperboloid embeded in $D+1$-dimenional Minkowski spacetime. Consider a hyperboloid:

$$-Z_0^2 + Z_1^2 + Z_2^2 + Z_3^2 + Z_4^2 = H_\Lambda^{-2} \tag{2.1}$$

embedded in 5d Minkowski space with metric:

$$ds_5^2 = dZ_0^2 - dZ_1^2 - dZ_2^2 - dZ_3^2 - dZ_4^2 \tag{2.2}$$

This hyperboloid lies outside the light cone and so the induced metric has Lorentzian signature.

To obtain an closed de Sitter universe, consider coordinates $\{t, \chi, \theta, \phi\}$ on the hyperboloid with transformation:

$$\begin{aligned} Z_0 &= H_\Lambda^{-1}\mathrm{sinh}(\mathrm{H}_\Lambda \mathrm{t}) \\ Z_1 &= H_\Lambda^{-1}\mathrm{cosh}(\mathrm{H}_\Lambda \mathrm{t})\mathrm{cos}\chi \\ Z_2 &= H_\Lambda^{-1}\mathrm{cosh}(\mathrm{H}_\Lambda \mathrm{t})\mathrm{sin}\chi\mathrm{cos}\theta \\ Z_3 &= H_\Lambda^{-1}\mathrm{cosh}(\mathrm{H}_\Lambda \mathrm{t})\mathrm{sin}\chi\mathrm{sin}\theta\mathrm{cos}\phi \\ Z_4 &= H_\Lambda^{-1}\mathrm{cosh}(\mathrm{H}_\Lambda \mathrm{t})\mathrm{sin}\chi\mathrm{sin}\theta\mathrm{sin}\phi \end{aligned} \tag{2.3}$$

We immediately get

$$ds^2 = dt^2 - H_\Lambda^{-2}\mathrm{cosh}^2(\mathrm{H}_\Lambda \mathrm{t})\left[\mathrm{d}\chi^2 + \mathrm{sin}^2\chi(\mathrm{d}\theta^2 + \mathrm{sin}^2\theta \mathrm{d}\phi^2)\right] \tag{2.4}$$

Another choice of coordinates reduce the metric in $\{Z_i\}$ coordinates to a form corresponding to an open de Siter universe:

$$\begin{aligned} Z_0 &= H_\Lambda^{-1}\mathrm{sinh}(\mathrm{H}_\Lambda \mathrm{t})\mathrm{cosh}\chi \\ Z_1 &= H_\Lambda^{-1}\mathrm{cosh}(\mathrm{H}_\Lambda \mathrm{t}) \\ Z_2 &= H_\Lambda^{-1}\mathrm{sinh}(\mathrm{H}_\Lambda \mathrm{t})\mathrm{sinh}\chi\mathrm{cos}\theta \\ Z_3 &= H_\Lambda^{-1}\mathrm{sinh}(\mathrm{H}_\Lambda \mathrm{t})\mathrm{sinh}\chi\mathrm{sin}\theta\mathrm{cos}\phi \\ Z_4 &= H_\Lambda^{-1}\mathrm{sinh}(\mathrm{H}_\Lambda \mathrm{t})\mathrm{sinh}\chi\mathrm{sin}\theta\mathrm{sin}\phi \end{aligned} \tag{2.5}$$

which leads to:

$$ds^2 = dt^2 - H_\Lambda^{-2}\mathrm{sinh}^2(\mathrm{H}_\Lambda \mathrm{t})\left[\mathrm{d}\chi^2 + \mathrm{sinh}^2\chi(\mathrm{d}\theta^2 + \mathrm{sin}^2\theta \mathrm{d}\phi^2)\right] \tag{2.6}$$

For the flat slicing, we do the transformation:

$$\begin{aligned} Z_0 &= H_\Lambda^{-1}\mathrm{sinh}(\mathrm{H}_\Lambda \mathrm{t}) + \mathrm{r}^2 \mathrm{e}^{\mathrm{H}_\Lambda \mathrm{t}} \mathrm{H}_\Lambda/2 \\ Z_1 &= H_\Lambda^{-1}\mathrm{cosh}(\mathrm{H}_\Lambda \mathrm{t}) - \mathrm{r}^2 \mathrm{e}^{\mathrm{H}_\Lambda \mathrm{t}} \mathrm{H}_\Lambda/2 \\ Z_2 &= e^{H_\Lambda t}\mathrm{sin}\chi\mathrm{cos}\theta \\ Z_3 &= e^{H_\Lambda t}\mathrm{sin}\chi\mathrm{sin}\theta\mathrm{cos}\phi \\ Z_4 &= e^{H_\Lambda t}\mathrm{sin}\chi\mathrm{sin}\theta\mathrm{sin}\phi \end{aligned} \tag{2.7}$$

And the metric is:

$$ds^2 = dt^2 - H_\Lambda^{-2}\mathrm{exp}(2\mathrm{H}_\Lambda \mathrm{t})\left[\mathrm{d}\chi^2 + \chi^2(\mathrm{d}\theta^2 + \mathrm{sin}^2\theta \mathrm{d}\phi^2)\right] \tag{2.8}$$

Actually, the exponential growth of the scale factor with time is what has been observed on large scales, studying Type I supernovae and other phenomenon.

2.2 Via analytical continuation

dS_D is a Lorentzian signature version of the Euclidean sphere S_D by analytic continuation:

$$Z_0 \to iZ_{D+1}, t \to i\tau \tag{2.9}$$

To see how analytic continuation changes the signature of the metric, consider the line elements of three surface with constant curvature:

$$d\Omega_3^2 = H_\Lambda^{-2}\left[d\chi^2 + \begin{pmatrix} \sinh^2\chi \\ \chi^2 \\ \sin^2\chi \end{pmatrix} d\Omega_2^2\right] \tag{2.10}$$

From top to bottom are metric with negative curvature, zero curvature and positive curvature.

The line elements for four dimensional case (with positive curvature) is:

$$dl_{4d}^2 = H_\Lambda^{-2}\left(d\xi^2 + \sin^2\xi \mathrm{d}\Omega_3^2\right) \tag{2.11}$$

Since de Sitter spacetime is of constant positive curvature, for $d\Omega_3$ we choose the bottom expression which is a three sphere (because only three sphere corresponds to positive curvature). After changing the variable $\xi \to H_\Lambda \xi$, the metric is recasted as

$$ds^2 = -dl_{4d}^2 = -d\xi^2 - H_\Lambda^{-2}\sin^2(\mathrm{H}_\Lambda\xi)\left[\mathrm{d}\chi^2 + \sin^2\chi(\mathrm{d}\theta^2 + \sin^2\theta \mathrm{d}\phi^2)\right] \tag{2.12}$$

This is the metric of positive curvature space in Euclidean signature. In order to obtain a metric of a close de Sitter spacetime in Lorentzian signature, one needs to apply the analytical continuation $\xi \to it + \pi/2$, which turns $\sin(\mathrm{H}_\Lambda\xi) \to \cosh(\mathrm{H}_\Lambda \mathrm{t})$:

$$ds^2 = dt^2 - H_\Lambda^{-2}\cosh^2(\mathrm{H}_\Lambda\mathrm{t})\left[\mathrm{d}\chi^2 + \sin^2\chi(\mathrm{d}\theta^2 + \sin^2\theta \mathrm{d}\phi^2)\right] \tag{2.13}$$

For an open de Sitter metric, we should analytically continue $\xi \to it$ and $\chi \to i\chi$ simultaneously, which turns $\sin(\mathrm{H}_\Lambda\xi) \to \mathrm{isinh}(\mathrm{H}_\Lambda\mathrm{t})$ and $\sin\chi \to \mathrm{isinh}\chi$:

$$ds^2 = dt^2 - H_\Lambda^{-2}\sinh^2(\mathrm{H}_\Lambda\mathrm{t})\left[\mathrm{d}\chi^2 + \sinh^2\chi(\mathrm{d}\theta^2 + \sin^2\theta \mathrm{d}\phi^2)\right] \tag{2.14}$$

Now we can demonstrate that this geometry solves Einstein's equations with a positive cosmological constant. In the vacuum, we have

$$R_{\mu\nu} - \frac{1}{2} g_{\mu\nu} R - \lambda g_{\mu\nu} = 0 \tag{2.15}$$

We find that with the de Sitter metric, if we compute the Riemann tensors and Riemann scalar then we get

$$\lambda = 2 - \cot^2\chi \mathrm{sech}^2 \mathrm{t} + \tanh^2 \mathrm{t} \tag{2.16}$$

which is greater than 0, thus the cosmological constant is positive.

Chapter 3

Constraints on Classical de Sitter Solution

3.1 Introduction

Since a small positive cosmological constant seems to be required by recent data, and also the universe went through a period of exponential expansion at a time shortly after the big bang, de Sitter space seems likely to play an important role in any understanding of our present and past universe. However, as we previously argued de Sitter space has no S Matrix, which is the only rigorously defined object in string theory. In this chapter we will study the statement of constructing an S matrix for large occupation numbers in initial and final states, and give an alternative to requiring the existence of an S matrix in the case of de Sitter space. We then study the challenge of searching a positive vacuum solution from an effective action within a controlled

approximation.

3.2 The S Matrix and Classical Field Evolution

Much of our focus will be on the evolution of classical perturbations in metastable de Sitter space. We will argue that many of these perturbations evolve towards a big crunch singularity, and that this is outside of the scope of current methods in string theory/quantum gravity. In critical string theory, the object of interest is the S matrix. A *classical* solution of the string equations corresponds to a space-time for which one can define a sensible scattering matrix. The connection to classical scattering, in field theory and string theory, arises from considering the evolution of small disturbances. These correspond to initial *and final* isolated, localized states, with large occupation numbers. These can be considered as coherent states. For a single real scalar field, for example, one can develop a classical perturbation theory. Start, at lowest order, with a field configuration of the form

$$\phi(x) = \phi_{\vec{p}_1}(x) + \phi_{\vec{p}_2}(x) + \phi_{\vec{k}_1}(x) + \phi_{\vec{k}_2}(x) \tag{3.1}$$

where each term represents a localized wave packet with mean momentum $\vec{k}_i$. Momentum conservation requires $\vec{p}_1 + \vec{p}_2 = \vec{k}_1 + \vec{k}_2$ within the momentum uncertainty, and non-trivial scattering requires that the wave packets all overlap at a point in space-time. Quantum mechanically, the scattering problem we have outlined here corresponds to some large number of particles of each momentum in both the initial and final states.

Making a decomposition into positive and negative frequency components:

$$\phi(x) = \phi^+(x) + \phi^-(x) \to \begin{cases} \phi^+(x)|\Phi\rangle = \Phi(x)|\Phi\rangle \\ \\ \langle\Phi|\phi^-(x) = \langle\Phi|\Phi^*(x) \end{cases} . \tag{3.2}$$

In momentum space, $\Phi^{\pm}(\vec{k})e^{i\vec{k}\cdot\vec{x}\mp i\omega t}$ corresponds to the positive and negative frequency components. Reality requires $\Phi^{\pm}(\vec{k}) = \Phi^{\pm *}(-\vec{k})$. Occupation numbers scale as $|\Phi^{\pm}(\vec{k})|$.

Order by order in the interaction, $\lambda\phi^4$, we can compute corrections to the classical scattering,

$$\delta\phi(x) = \delta\phi_{\vec{p}_1}(x) + \delta\phi_{\vec{p}_2}(x) + \delta\phi_{\vec{k}_1}(x) + \delta\phi_{\vec{k}_2}(x). \tag{3.3}$$

Evaluated at the interaction point, $\delta\phi$ defines an S matrix (more precisely a T matrix) on the space of coherent states. This can be decomposed as an S matrix on states of definite particle number; the classical approximation is valid when the occupation numbers are large.

Phrased this way, the statement that one can construct an S matrix for large occupation numbers in initial and final states is the statement that one has sensible evolution from any initial classical configuration (described by $\vec{p}_1, \vec{p}_2$) to any final configuration $(\vec{k}_1, \vec{k}_2)$.

In the case of de Sitter space, the question of the existence of an S matrix is subtle [26]. We will focus, instead, on what we view as a minimal requirement that all classical perturbations in a would-be metastable de Sitter vacuum have a sensible evolution arbitrarily far into the future. We will see that some subset of possible perturbations evolve to singular geometries, over which we have no theoretical control. We

argue that this means that one does not have a controlled construction of such spaces. The existence, or not, of such metastable de Sitter spaces then becomes a matter of conjecture.

3.3 Searching for Stationary Points of an Effective Action

We first explore some of the challenges to the construction of stationary points of the effective action with positive c.c. Typically, these efforts involve the introduction of branes, orientifold planes, and fluxes [9]. One searches for particular stationary points of the action with positive cosmological constant, and asks whether the string coupling is small and the compactification radii large at these points [27, 28]. This, by itself, does not address the question of whether there is a systematic approximation. The system with branes and fluxes is not a small perturbation of the system without, and the range of validity of the expansion in one is not related to that of the other. If there is to be a systematic approximation of any sort, one requires a sequence of such stationary points as one increases the flux numbers; the would-be small parameters are the inverse of some large flux numbers. In our discussion we will assume that it makes sense to take such numbers arbitrarily large. Then the goal is to find stable, stationary points of the action where

1. The string coupling is small.

2. All compactification radii are large.

3. The cosmological constant is small and positive.

As reviewed in [10], satisfying this set of constraints is challenging. We review some of the issues in this section. Similar analyses, with similar conclusions, have appeared in [11–13]. Our point of view is that this is not surprising. Searches at weak coupling were not likely to yield non-supersymmetric metastable vacua, dS or AdS, and provide little information about the existence or non-existence of such states. For the dS case, it is hard to see how such states could be understood without a much broader understanding of their cosmology, as we will discuss subsequently.

We follow [9] in studying type II theories in the presence of an O_p plane, and a background geometry with metric

$$ds^2 = g_{\mu\nu} dx^\mu dx^\nu + \rho\ g^0_{IJ}\ dy^I dy^J. \tag{3.4}$$

Here g^0_{IJ} represents a background reference metric for the compactified dimensions. $g_{\mu\nu}$ represents the metric of four dimensional space-time, which we hope to be de Sitter. Reference [9] distinguishes directions parallel and perpendicular to the orientifold plane with an additional modulus σ; for simplicity, we assume $\sigma \sim 1$; this assumption can be relaxed without severe difficulty. We ignore other light moduli as well. We also include NS-NS 3-form and R-R q-form fluxes, $H^{(n)}_{IJK},\ F^{(n)}_q$.

The fluxes will be understood as taking discrete, quantized values. The dependence of terms on the moduli ρ and $\tau = \rho^{3/2}\ e^{-\phi}$ is given in [9], and is readily understood from the following considerations:

1. In the NS-NS sector, there is a factor $1/g^2 = e^{-2\phi}$ in front of the action. The four-dimensional Einstein term has a coefficient $\tau^2 = \rho^3/g^2$. This can be brought

to canonical form by the Weyl rescaling, $g_{\mu\nu} \to g_{\mu\nu}\tau^{-2}$. The moduli τ and ρ will be our focus.

2. Again in the NS-NS sector, terms involving the three-index tensor, before rescaling, contain a factor $\tau\rho^{-3}$; after the Weyl rescaling, they acquire an additional factor of τ^{-3} in front. Terms involving the six-dimensional curvature similarly scale as $\rho^{-1}\tau^{-3}$.

3. In the RR sector, the flux terms have, before rescaling, no factors of $1/g$. They have various factors of ρ depending on the rank of the tensor. The Weyl rescaling introduces a factor of τ^{-4}.

The resulting action is [9]:

$$V = -\tau^{-2}\left(\rho^{-1}R_6(\sigma) - \frac{1}{2}\rho^{-3}\sum_n \sigma^{6n-3(p-3)}\left|H^{(n)}\right|^2\right) - \tau^{-3}\rho^{\frac{p-6}{2}}\sigma^{\frac{(p-3)(p-9)}{2}}\frac{T_{10}}{p+1}$$
$$+\frac{1}{2}\left(\tau^{-4}\sum_{q=0}^{4}\rho^{3-q}\sum_n \sigma^{6n-q(p-3)}\left|F_q^{(n)}\right|^2 + \frac{1}{2}\tau^{-4}\rho^{-2}\sum_n \sigma^{6n-5(p-3)}\left|F_5^{(n)}\right|^2\right). \tag{3.5}$$

Compare $R_6(\sigma)$ and T_{10} term, since $R_6(\sigma) \sim 1$ and $T_{10} \sim 1$, then the condition of T_{10} term dominates is

$$\tau^{-2}\rho^{-1} \ll \tau^{-3}\rho^{\frac{p-6}{2}} \tag{3.6}$$

With the Weyl rescaling $\tau \sim \frac{1}{g_s}\rho^{3/2}$, we find that when $p = 8$, T_{10} term will dominate R_6 term. For $p = 3, 4, 5, 6, 7$, R_6 term will dominate T_{10} term. Again, we will ignore the index (n) in what follows and set $\sigma = 1$. To illustrate the issues, we will first consider large F_2 and F_4 which correspond to Type IIA string theory. These fluxes satisfy, with

$H_3 = 0$, Bianchi identities, with a source for F_4. These equations can be satisfied with large fluxes through two and four cycles.

For $3 \leq p \leq 7$ and choosing $T_{10} = 1$, $R_6 \sim 1$, we can drop the T_{10} term because the R_6 term will dominate. We can attempt to find large τ and ρ by turning on $F_2 = n_2$ and $F_4 = n_4$ (other combinations of fluxes give similar results). Then one has the relevant terms:

$$-\tau^{-2}\rho^{-1}R_6 + \frac{1}{2}\tau^{-4}\left(n_2^2\rho + n_4^2\rho^{-1}\right). \tag{3.7}$$

Differentiating with respect to ρ and τ, for $n_4 \gg n_2 \gg 1$, one has then

$$\rho^{-2}R_6 + \frac{1}{2}\tau^{-2}\left(n_2^2 - n_4^2\rho^{-2}\right) = 0 \tag{3.8}$$

and

$$\rho^{-1}R_6 - \tau^{-2}\left(n_2^2\rho + n_4^2\rho^{-1}\right) = 0. \tag{3.9}$$

We get a solution of the form:

$$\rho^2 = -\frac{1}{3}\left(\frac{n_4}{n_2}\right)^2;\ \tau^2 = \frac{2}{3}\frac{n_4^2}{R_6}. \tag{3.10}$$

Negative ρ^2 is not acceptable. But even if somehow ρ^2 had been positive, we would have had:

$$g^2 = \frac{\rho^3}{\tau^2} \propto R_6\left(\frac{n_4}{n_2^3}\right); \tag{3.11}$$

so the string coupling would not have been weak. The other terms we have neglected are suppressed at this point. For example, the term proportional to $T_{10}\rho^{-3/2}\tau^{-3}$ is suppressed by $(n_2/n_4)^2$.

For $p = 8$, which corresponds to the T_{10} term dominating, turning on, again, n_4 and n_2, one finds that $\rho^2 = -7n_4^2/n_2^2$, which is also negative. Parameterically, one now has $g^2 \propto n_4^3/n_2^7$, so again, even if one ignored signs, this regime would give large ρ and τ but also large g.

An interesting case is provided by $p = 8$ with n_0 and n_2 non-zero. In this case, one finds that

$$\rho^2 = \frac{1}{5}\frac{n_2^2}{n_0^2} \; ; \quad \tau = \frac{8}{5}n_2^2 \tag{3.12}$$

so one requires $n_2 \gg n_0$. Both quantities are now positive, but the cosmological constant, consistent with expectations of [9], is negative, corresponding to AdS space. Setting this aside, one has that

$$g_s^2 \propto \frac{1}{n_2^2} \tag{3.13}$$

so the string coupling is small. But this is not good enough. If one considers higher derivative terms in the effective action at tree level (α' expansion) these are not suppressed. Writing the action in ten dimensions, the terms (written schematically)

$$\int d^4x d^6y \sqrt{g_4}\sqrt{g_6}\left(F_{IJ}F^{IJ} + \left(F_{IJ}F^{IJ}\right)^2\right) \tag{3.14}$$

are both of the same order in the large flux, n_2^2, due to the two extra factors of ρ^{-2} coming from the two extra powers of inverse metric in the second term. For all values of p, if we just consider the H and F_q terms, $\partial V/\partial\tau = 0$ gives negative ρ^2.

In other cases, one finds these and other pathologies—AdS rather than dS stationary points and instabilities. Searches involving broader sets of moduli [27, 28] seem to allow at best a few isolated regions of parameter space where such solutions

might exist. Whether these might exhibit a sensible perturbation expansion is currently an open question, but our results above suggest that the combination is a tall order. So, even with the large freedom in flux choices we have granted ourselves, metastable de Sitter stationary points would appear far from generic in regimes where couplings are small and compactification radii are large.

Chapter 4

The Challenge of Cosmological Solutions

4.1 Introduction

One severe limitation of string theory is that it is unable to describe cosmologies resembling our own which appear to emerge from a big bang singularity, and similarly cosmologies which evolve to a big crunch. Here we will show that given a effective potential in string theory where there is a de Sitter vacuum at some $\Phi = \Phi_0$, and the absolute minimum occurs at $\Phi = \infty$ with exactly zero vacuum energy, if we start the system with expanding/contracting boundary conditions then the universe will evolve to a big bang/crunch singularity in the further past/future.

4.2 Expectations for Evolution of Perturbations in de Sitter Space

String theory has had many dramatic successes in understanding issues in quantum gravity. But one severe limitation is its inability, to date, to describe cosmologies resembling our own, which *appear* to emerge from a big bang singularity or evolve to a big crunch singularity. This could reflect some fundamental limitation; more likely, it reflects the inadequacy of our present theoretical tools to deal with situations of high curvature and strong coupling. For example, consider a pseudomoduli space where the potential falls to zero for large fields in the positive direction. If one starts the system in the far past with expanding boundary conditions, then further in the past there is a big bang singularity; if one starts with contracting boundary conditions, there is a big crunch in the future [29]. These high curvature/strong coupling regions are inevitable, despite the system being seemingly weakly coupled through much of this history. It is possible that in any string cosmology, there need not be an actual curvature singularity, but the growth of the curvature means that the system enters a regime where any conventional sort of effective action or conventional weak coupling string description breaks down. It seems hard to avoid the conclusion that there is such a singularity (regime of high curvature) in the past or future of cosmological solutions on a moduli space. These problems might be avoided in some more complete treatment of the problem within the framework of a single cosmology, or perhaps something else, such as eternal inflation in a multiverse, is needed. In any case, the problem is beyond our present theoretical

reach.

Our question, in this section, is: *are things better for metastable de Sitter space-times*? In particular, in efforts to construct de Sitter space-times in string theory, the strategy is to search some effective action for a positive c.c. stationary point, separated by a finite potential barrier from a region in field space where, asymptotically, the potential tends to zero. If we start the system at the local minimum of the potential, classically, it will stay there eternally. But how do small fluctuations evolve? Might there be small disturbances that drive the field to explore the region on the other side of the barrier, exhibiting the pathologies of the system on pseudomoduli spaces of [29]?

In one presentation of de Sitter space (which covers all of the space):

$$ds^2 = -d\tau^2 + \cosh^2(H\tau)\left[d\chi^2 + \sin^2\chi d\Omega_2^2\right]. \tag{4.1}$$

A homogeneous scalar field in this space, $\phi(\tau)$, obeys

$$\ddot{\phi} + 3H\frac{\sinh(H\tau)}{\cosh(H\tau)}\dot{\phi} + V'(\phi) = 0. \tag{4.2}$$

The equation is slightly more complicated if ϕ depends on r as well.

The metric of equation 4.1 respects an $SO(4,1)$ symmetry, as well as a Z_2 that reverses the sign of τ. Suppose, first, the potential for ϕ rises in all directions about a minimum (taken at $\phi = 0$ for simplicity). For large positive τ, any perturbation of ϕ about a local minimum damps; for large negative τ, the motion is amplified as τ increases (it damps out in the past). Correspondingly, in the far past and the far future, the field approaches the local minimum (to permit a perturbative discussion, we must require that the maximum value of the disturbance at all times is small). Starting in the

far past, we can think in terms of a localized disturbance in space (e.g., due to a source localized in space time) and study the Fourier transformed field. If the disturbance has some characteristic momentum k, this momentum will blueshift exponentially as $\tau \to 0$, and the amplitude will grow. For $\tau > 0$, the distribution will damp and redshift to longer wavelengths.

If the perturbation has scale smaller than H^{-1} (and in particular if the Hubble constant is small compared to the curvature of the potential), then the space-time near the disturbance is approximately flat, and, assuming rotational invariance, the disturbance breaks $SO(3,1) \times$ translations to $SO(3)$. In terms of the full symmetry of de Sitter space, the perturbation breaks $SO(4,1)$ to $SO(3)$. To summarize, any approximately homogeneous disturbance in eternal de Sitter corresponds to a solution that grows in the far past and decreases in the future. One can define *past* and *future* relative to the point where the scalar field is a maximum. The location of this point breaks much of the continuous symmetry of de Sitter space but leaves $SO(3) \times Z_2$, where the Z_2 represents time reversal about the point where the amplitude of the field oscillation is a maximum. The maximum of the field, indeed, provides a natural definition of the origin of time. At this point, the time derivative of the field vanishes.

Now for a potential that has a local minimum with positive energy density, and that falls to zero for large $|\phi|$, we might expect that if we create a small, localized perturbation at some (r_0, τ_0) this perturbation will damp out if $\tau_0 \gg 0$. But if $\tau_0 \ll 0$, the perturbation will grow, possibly crossing over the barrier while $\tau \ll 0$. In this case, the emergent universe on the other side of the barrier is contracting, and we might

expect the system to run off towards $\phi = \infty$, until the universe undergoes gravitational collapse. If this is the case, then the Z_2 symmetry might be said to be spontaneously broken; one has a pair of classical solutions, one with a singularity in the past, one in the future, related by the Z_2 symmetry.

Before establishing this fact, it is helpful to review some aspects of the Coleman-De Luccia (CDL) bounce from this perspective [30].

4.2.1 The Coleman-De Luccia bounce as a solution of the field equations with Minkowski signature

We are interested in disturbances which lead to motion over a barrier, rather than tunneling. We might expect, however, that once the system passes over the barrier, its subsequent evolution is not particularly sensitive to whether it passed over the barrier or tunneled through it. In the case of a thin-wall bubble, before including gravity, at large times, the bubble wall becomes relativistic, and the bubble radius is of order t, so one expects that the bubble energy is proportional to t^3, dwarfing any difference in the energy of order the barrier height at the time of bubble formation. The same is true for a thick-walled bounce connecting two local minima of some potential. In other words, at large time, at least for very small G_N, we might expect the solution to be a small perturbation of the bounce solution of Coleman [31] and Coleman and De Luccia [30], which we will review briefly.

4.2.2 Tunneling with $G_N = 0$

Consider, first, the bounce solution without gravity. We consider a potential, $V(\phi)$, with local minima at $\phi_{\text{true}},\ \phi_{\text{false}}$, where $V(\phi_{\text{false}}) > V(\phi_{\text{true}})$. Starting with the field equations,

$$\Box\Phi + V'(\phi) = 0, \tag{4.3}$$

for points that are space-like separated from the origin (the center of the bubble at the moment of its appearance), we introduce $\xi^2 = r^2 - t^2$, in terms of which

$$\frac{d^2\phi}{d\xi^2} + \frac{3}{\xi}\frac{d\phi}{d\xi} - V'(\phi) = 0. \tag{4.4}$$

This is the Euclidean equation for the bounce.

For points that are time-like separated, calling $\tau^2 = t^2 - r^2$,

$$\frac{d^2\phi}{d\tau^2} + \frac{3}{\tau}\frac{d\phi}{d\tau} + V'(\phi) = 0. \tag{4.5}$$

These equations are related by $\xi = i\tau$.

On the light cone, $\xi = \tau = 0$, we have $d\phi/d\tau = d\phi/d\xi = 0$, and we have to match $\phi(0) = \phi_0$. In the tunneling problem [31], ϕ_0 is determined by the requirement that $\phi \to \phi_{\text{false}}$ as $\xi \to \infty$; this can be thought of as a requirement of finite energy relative to the configuration where $\phi = \phi_{\text{false}}$ everywhere.

Independent of the quantum mechanical tunneling problem, the bounce is a solution of the source-free field equations for all time (positive and negative) and everywhere in space. In the time-like region, the solution for negative time is identical to that for positive time. Translation invariance is broken, but $SO(3,1)$ invariance and the Z_2 invariance are preserved.

4.2.3 Classical perturbations of the false vacuum with $G_N = 0$

Without gravity, we might consider starting the system in the false vacuum and giving it a "kick" so that, in a localized region, the system passes over the barrier. On the other side, the system looks like a bubble, but not of the critical size. We might expect that the evolution of the bubble, on macroscopic timescales, is not sensitive to the detailed, microscopic initial conditions. For a thin-walled bubble, for example, we can think of configurations, as in [31], where at time $t = 0$, one has a bubble of radius R_0, inside of which one has true vacuum, outside false vacuum, and a transition region described by the kink solution of the one dimensional field theory problem with nearly degenerate minima. Take the case of a single real field, ϕ, with potential:

$$V(\phi) = -\frac{1}{2}\mu^2\phi^2 + \frac{1}{4}\lambda\phi^4 + \epsilon\phi + V_0.$$

For small ϵ, the minima of the potential lie at

$$\phi_\pm \approx \pm\sqrt{\frac{\mu^2}{\lambda}}. \tag{4.6}$$

We can define our bubble configuration, with radius R large compared μ^{-1}, as the kink solution of the one dimensional problem,

$$\phi_B(r;R) = \frac{\phi_+ - \phi_-}{2}\tanh\left(\frac{\mu(r-R)}{\sqrt{2}}\right) + \frac{\phi_+ + \phi_-}{2}. \tag{4.7}$$

For our problem, we want to treat $R \to R(t)$ as a dynamical variable. If $R_0(t)$ is slowly varying in time (compared to μ^{-1}), then we can write an action for R,

$$S = \int dt \int r^2 dr d\Omega \left(\frac{1}{2}(\partial_t\phi_B(r;R(t)))^2 - (\vec{\nabla}\phi_B(r,R(t)))^2 - V(\phi_B(r,R(t)))\right) \tag{4.8}$$

$$\approx \int dt 4\pi R^2 \int_{R-\delta}^{R+\delta} dr \left(\frac{1}{2}(\partial_r \phi)^2\right)\left(\dot{R}^2 - 2\right),$$

where we have used the thinness of the wall to reduce the three-dimensional integral to a one-dimensional integral, and the fact that for the kink solution, the kinetic and potential terms are equal, to write the second term. We will restore the ϵ term in a moment.

The integral over the bounce solution is straightforward, yielding $\sqrt{2/3}$. So we have the effective action for R,

$$S = 4\pi \int dt \left(\sqrt{\frac{2}{3}}\mu^3(R^2\dot{R}^2 - 2R^2) + \frac{\epsilon}{3}R^3\right). \tag{4.9}$$

Correspondingly, the energy of the configuration is:

$$E(R,\dot{R}) = 4\pi\left(\sqrt{\frac{2}{3}}(R^2\dot{R}^2 + 2R^2 - \frac{1}{3}\epsilon R^3)\right) \equiv \frac{M(R)}{2}\dot{R}^2 + V(R). \tag{4.10}$$

We can extract several results from this expression. In particular we have:

1. The point where the potential vanishes, $R = R_1 = \frac{2\sqrt{2}\mu^3}{\epsilon}$.

2. The location and value of the potential at the maximum: $R = R_2 = \frac{4\sqrt{2}\mu^3}{3\epsilon}$.

3. We can determine $\dot{R}$ as a function of R and the initial value of R (for simplicity assuming $\dot{R}(0) = 0$).

We have checked, numerically, that starting with a field configuration corresponding to $\phi(x, t = 0) = \phi_B(r; R)$, $\dot{\phi}(x, t = 0) = 0$, to the left of the barrier, the bubble collapses. Starting slightly to the right, the wall quickly becomes relativistic

and expands. This is consistent with an intuition that the energy of conversion of false vacuum to true is largely converted into the energy of the wall.

We can make this latter statement more precise. If we write:

$$\phi(r,t) = \phi_{\rm cr}(t,r) + \chi(t,r), \qquad |\chi| \ll \phi_{\rm cr}, \tag{4.11}$$

where $\phi_{\rm cr}$ is the critical bubble solution, then

$$(\partial^2 + m^2(r,t))\chi = 0. \tag{4.12}$$

Here m^2 is essentially a θ function, transitioning between the mass-squared of χ in the false and true vacua. Since the bubble wall moves at essentially the speed of light, and undergoes a length contraction by $t \sim \gamma$, we have that

$$m^2(t,r) \approx m^2(t^2 - r^2) \tag{4.13}$$

and the χ equation is solved by

$$\chi = \frac{1}{r}\chi(t^2 - r^2). \tag{4.14}$$

So the amplitude of χ decreases with time, and the energy stored is small compared to that in the bubble wall.

We expect the same to hold for a thick-walled bounce.

4.2.4 Behavior of the disturbance with small G_N

Consider the same system, now with a small G_N. Again, our disturbance, after a short period of time, approaches the critical ($G_N = 0$) bubble. At larger time, it will then agree with the Coleman-De Luccia solution, including the small effects of gravity.

As we will see in the next section, for the asymptotically falling potential, with expanding boundary conditions, the evolution of the configuration is non-singular. But with contracting boundary conditions, one encounters, as expected, a curvature singularity.

4.3 Behavior of the Bounce with Asymptotically Falling Potential

We have argued that, independent of the microscopic details of the initial conditions, in the case of a disturbance that connects two metastable minima of a scalar potential, the large time evolution of an initial disturbance that crosses the barrier is that of the critical bubble, in the limit of small G_N. We expect that the same is true for a potential that falls asymptotically to zero. Once more, the underlying intuition is that at late times, the energy released from the change of false to true vacuum overwhelms any slight energy difference in the starting point. So we expect the solution to go over to $\phi(\tau)$. So in this section, we will focus principally on the behavior of the critical bubble, $\phi(\tau)$.

4.3.1 Field evolution with small G_N

For small but finite G_N, there is a long period where $G_N \times T_{00} \times \tau^2 \ll 1$, gravitation is negligible, and the picture of the previous section of the flat-space evolution of the bubble (or disturbance) is unaffected. For a vacuum bubble in de Sitter

space, gravitational effects become important, for fixed $r \ll H^{-1}$, for example, only once $t \sim H^{-1}$. Provided the bubble has evolved to a configuration approximately that of the critical bubble, we can take over the critical bubble results (with gravity).

So we consider the bubble evolution in the region of Minkowski signature. Writing the metric in the form

$$ds^2 = -d\tau^2 + \rho(\tau)^2 \left(d\sigma^2 + \sinh^2(\sigma) d\Omega_2^2 \right), \tag{4.15}$$

the equations for ρ and ϕ are:

$$\ddot{\phi} + 3\frac{\dot{\rho}}{\rho}\dot{\phi} + V'(\phi) = 0 \tag{4.16}$$

and

$$\dot{\rho}^2 = 1 + \frac{\kappa}{3}\left(\frac{1}{2}\dot{\phi}^2 + V(\phi) \right) \rho^2. \tag{4.17}$$

Note that if the bubble emerges in a region of large ρ ($\kappa\rho^2 V \gg 1$) then, for the asymptotically falling potential, the kinetic term quickly comes to dominate in the equation for ρ; the system becomes kinetic energy dominated. This is visible in the numerical results we describe subsequently.

We should pause here to consider the tunneling problem. We will see in the next section that if we take the positive root in equation 4.17, one obtains an expanding universe in the future, but there is a singularity in the far past (before the appearance of the bubble). Alternatively, if we take the negative root, the singularity appears in the far future. Which root one is to take brings us to questions of the long-time history of the universe, i.e., how the universe came to be in the metastable false vacuum. The point of our discussion in this paper is that this issue already arises classically.

4.3.2 Behavior of the equations for large τ

Before describing our numerical results, it is helpful to consider some crude approximations which give insight into the behavior of the system. In the region with $\xi = i\tau$, the equations become those of CDL in the time-like region:

$$\ddot{\phi} + 3\frac{\dot{\rho}}{\rho}\dot{\phi} + \frac{dV}{d\phi} = 0, \tag{4.18}$$

$$\dot{\rho} = \pm\sqrt{1 + \frac{\kappa}{3}\rho^2\left(\frac{1}{2}\dot{\phi}^2 + V(\phi)\right)}. \tag{4.19}$$

We argued at the end of the previous section that we might expect that the potential is not particularly relevant in the ϕ equation for large $\rho(0)$. Ignoring the potential, we can also ask, self consistently, whether the second term in the $\dot{\rho}$ equation dominates over the first. If it does, we have an FRW universe with $k = 0$ and

$$\rho \propto (\tau - \tau_0)^{1/3}, \quad \tau > \tau_0; \qquad \rho \propto (\tau_0 - \tau)^{1/3}, \quad \tau < \tau_0. \tag{4.20}$$

(These are the results for a universe with $p = w\rho;\ w = 1$.) We can see this directly from the equations. We have

$$\frac{\dot{\rho}}{\rho} = \pm\sqrt{\frac{\kappa}{6}}\dot{\phi}. \tag{4.21}$$

So

$$\frac{d^2\phi}{d\tau^2} \pm \sqrt{\frac{3\kappa}{2}}\dot{\phi}^2 = 0. \tag{4.22}$$

We look for a solution of the form

$$\dot{\phi} = \alpha(\tau - \tau_0)^{-1}, \tag{4.23}$$

$$\alpha = \sqrt{\frac{2}{3\kappa}}. \tag{4.24}$$

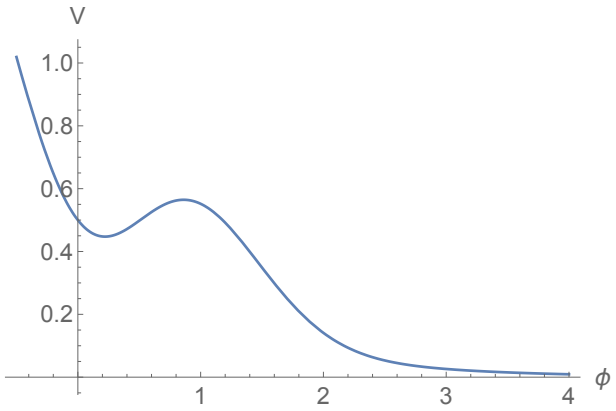

Figure 4.1: ϕ potential.

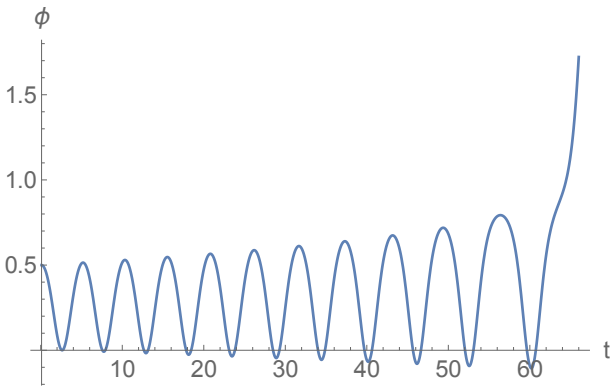

Figure 4.2: ϕ crosses the barrier.

Plugging this back into the $\dot{\rho}$ equation gives

$$\frac{\dot{\rho}}{\rho} = \pm\frac{1}{3}\frac{1}{\tau - \tau_0}, \tag{4.25}$$

which is consistent with the expected $(\tau - \tau_0)^{1/3}$ behavior. So we have a singularity in the past or the future.

For numerical studies, we designed a potential with a local de Sitter minimum

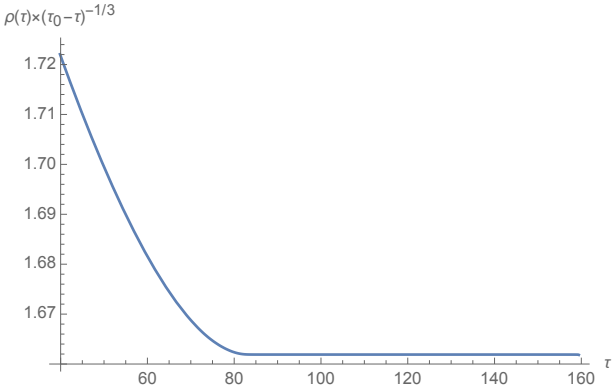

Figure 4.3: $\rho(\tau) \sim (\tau_0 - \tau)^{1/3};\ \tau_0 \approx 159.5.$

that tends to zero for large ϕ

$$V(\phi) = \frac{1}{2}e^{-\phi} + \phi^2 e^{-\phi^2}, \tag{4.26}$$

This is plotted in Figure 4.1; the local minimum lies near $\phi = 0.2$. The potential blows up for negative ϕ, but this will not concern us. We solve equations 4.18 and 4.19 with ϕ_0 taken to be not too far from the local minimum, with small $d\phi/d\tau$ and with the negative sign in the root of the ρ equation: $\phi(\tau = 0) = 1/2;\ \phi'(\tau = 0) = -10^{-6};\ \rho(\tau = 0) = 10$. One sees (Figure 4.2) the scalar field roll over the barrier after some number of oscillations. The ratio of potential to kinetic energy quickly tends to zero after the crossing. As we expect, we find a singularity at a finite time in the future, and indeed $\rho(\tau)$ behaves as $(\tau_0 - \tau)^{1/3}$ (Figure 4.3).

We have argued that for more general initial conditions, provided gravity is sufficiently weak, the system evolves quickly to the bounce configuration with $G_N \approx 0$. Its evolution will then be as above.

4.3.3 Implications of the singularity

Our main concern with the singularity is whether it is an obstruction to any sort of systematic analysis. If we have a weak coupling, small curvature description of the system, allowing a perturbative analysis, we expect to be able to write an effective Lagrangian including terms of successively higher dimension—higher numbers of derivatives—such as:

$$L = \sqrt{g}\left(\frac{1}{G_N}R + R^2 + \frac{1}{M^2}R^4 + \ldots + (\partial_\mu\phi)^2 + \frac{1}{M^4}(\partial_\mu\phi)^4\right).$$

If one tries to analyze the resulting classical equations perturbatively, in the presence of $\dot{\phi} \sim 1/(t-t_0)$ and $R \sim 1/(t-t_0)^2$, at low orders, the terms in the expansion diverge and the expansion breaks down. This is similar to the phenomena at a big bang or big crunch singularity.

Chapter 5

Discussion and Conclusions

We have argued, from two points of view, that one cannot construct de Sitter space in any controlled approximation in string theory. First, we have seen that even allowing the possibility of arbitrarily large fluxes, it is very difficult to find stationary points for which both the string coupling is small and compactification radii are large, even before asking whether the corresponding cosmological constant is positive or negative. We have seen that typically when sensible stationary points exist, even if formally radii are large and couplings small, higher order terms in the expansions are not small. Related observations have been made in [32], based on conjectures about the behavior of quantum gravity systems.

But our second obstacle seems even more difficult to surmount: a set of small perturbations of any would-be metastable de Sitter state, classically, will evolve to uncontrollable singularities.

This is *not* an argument that metastable de Sitter states do not exist in quan-

tum theories of gravity; only that they are not accessible to controlled approximations. The problem is similar to the existence of big bang and big crunch singularities; we have empirical evidence that the former exists in the quantum theory that describes our universe, but we do not currently have the tools to describe these in a quantum theory of gravity.

Reference [33] has considered the question from the perspective of the KKLT [6] constructions. These involve vacua with fluxes, but the small parameter is not provided by taking all fluxes particularly large; rather, it arises from an argument that there are so many possible choices of fluxes that in some cases, purely at random, there is a small superpotential. In other words, there is conjectured to be a vast set of (classically) metastable states of which only a small fraction permit derivation of an approximate four-dimensional, weak coupling effective action. Reference [33] argues that such a treatment is self consistent. We are sympathetic to the view that such an analysis provides evidence that if in some cosmology one lands for some interval in such a state, the state can persist for a long period. But a complete description of such a cosmology is beyond our grasp at present.

In considering the cosmic landscape, one of the present authors has argued that, even allowing for the existence of such states in some sort of semiclassical analysis, long-lived de Sitter vacua will be very rare, unless protected by some degree of approximate supersymmetry [34]. The breaking of supersymmetry would almost certainly be non-perturbative in nature; searches for concrete realizations of such states (as opposed to statistical arguments for the *existence* of such states, along the lines of KKLT) would

be challenging.

Ultimately, at a quantum level, reliably establishing the existence of metastable de Sitter space appears to be a very challenging problem. One needs a cosmic history, and it would be necessary that this history be under theoretical control, both in the past and in the future. As a result, the significance of failing to find stationary points of an effective action describing metastable de Sitter space is not clear. We have seen that even thought of as classical configurations, there are questions of stability and obstacles to understanding the system eternally, once small perturbations are considered. We view the question of the existence of metastable de Sitter space as an open one.

Part II

Transplanckian Censorship Conjecture

Chapter 6

Introduction

Here we will generally assume that the de Sitter Swampland conjecture is correct, and review and further explore some of its consequences. As discussed in [8], one of the most immediate is that the observed dark energy must be a form of quintessence. Quintessence requires equation of state parameter $w < -1/3$. Observations require w close to -1. Whether such configurations arise in string theory – with sensible scales of energy, mass scales for the Higgs, and so on – is an interesting (and extremely challenging) question, which we will not explore here. We will confine ourselves to a narrower question. Assuming that one has a landscape in string theory with quintessence like configurations as well as negative cosmological constant stationary points, then these states are unstable to decay to AdS spaces (more precisely to states of negative cosmological constant). Ref. [35] insisted on a criterion for sensible states. They noted that in these quintessence states, one has superluminal expansion. If the state lives long enough, Planck scale fluctuations will redshift until they become larger than the

horizon. The authors of [35] argued that this is not sensible, and that there should be a limit on the lifetime, Γ, of such states:

$$\Gamma < H \log(H). \tag{6.1}$$

While not committing ourselves to a view on this basic question of principle, we will ask: is this plausible? What are the lifetimes of such quintessence states likely to be? This will require that we consider some aspects of tunneling, from a state which is evolving in time towards zero energy, to a lower energy state. We will first consider this in quantum mechanics, and then in quantum field theory without gravity, and finally in a generally relativistic theory. In the first two cases, we will see that the lifetimes can be quite long. In fact, typically, there is a finite probability that the system never makes a transition to the lower state at all. These systems are not amenable to conventional WKB/Euclidean path integral approaches, but it is not difficult to make rough estimates of the tunneling rates working with Minkowski signature.

Including general relativity, and more generally in a would-be quantum theory of gravity, we are on less certain ground. In string theory, in the absence of supersymmetry, one might expect that states with potentials which fall to zero for large values of scalar ("pseudomoduli") fields are typical. Such potentials would go to zero at least exponentially rapidly in various regions of field space. We will generally model the tunneling problem by considering potentials which, in one direction direction, labeled by a field ϕ, are pure exponentials, $V(\phi) = Ae^{-\lambda\phi}$.[1] There is another direction, χ, such

[1] In terms of fields with canonical kinetic terms, potentials might well be expected to tend to zero far more rapidly.

that at some point, there is a local minimum with negative c.c. for both λ and χ. As we will review, in the first regime, unless the coefficient in the exponential satisfies a certain bound, the potential quickly becomes negligible and one has a universe with $p = \rho$, i.e. $w = 1$. The TCC does not constrain these systems. For sufficiently small λ, the system may exhibit quintessence. We will focus our considerations on such states. We will argue that tunneling is highly suppressed, as in the non-gravitational case.

Chapter 7

The de Sitter Swampland And Trans Planckian Censorship Conjectures

The vacuum states we can claim to understand in string theory generally possess a high degree of supersymmetry. States without supersymmetry, especially de Sitter space (or flat space) are hard to access by weak coupling methods[7]. Indeed, as stressed in [36], typical non-supersymmetric states exhibit runaway to singular spacetimes and strong coupling, and one cannot claim to understand these in any systematic way. Such states might be candidates for quintessence. That said, the work of Bousso and Polchinski[5] and KKLT[6] suggests the possible existence of a landscape of states, with a discretuum of positive and negative cosmological constants. The existence of these states can hardly be viewed as rigorously established. Ooguri and Vafa[32] conjectured, based on the difficulty of finding dS stationary points of effective potentials of systems with branes and fluxes[9], that de Sitter vacua, stable or unstable, may not

exist, and that the presently observed dark energy is a form of quintessence. In [36], it was demonstrated that there are fundamental obstacles to weak coupling searches, and argued that these don't provide an argument, one way or the other, about the existence of metastable de Sitter space in string theory/quantum gravity. The work of that reference focused heavily on the fact that such would-be states are metastable, and in the past or future, the space-time becomes singular at the classical level.

In [35], Bedroya and Vafa set forth an additional conjecture. They argued that Planck scale fluctuations should not become classical. So for any would-be state, the lifetime, T, should satisfy

$$T < H_f^{-1} \log H_f, \tag{7.1}$$

where H_f is the Hubble parameter at the moment of decay.

If a landscape picture holds, any quintessence vacuum will be surrounded by classically stable, negative cosmological constant stationary points. As the quintessence field roles in its potential, it can decay to one of these stable minima, but we would expect that the decay amplitude would rapidly get smaller as the field ϕ rolls down its hill. This is a slightly unconventional tunneling problem, and we will consider it first in a quantum mechanics system with two degrees of freedom, and then in field theory without general relativity, before attacking the actual problem of interest. In both of these cases, we will find significant suppression of the decay amplitude. Turning to the gravitational case with quintessence, we lack an explicit, controlled string model. Still, it would seem that if such systems exist, lifetimes, for large values of teh quintessence field/small values of the energy density are likely to be very long, violating the conjecture. So there would

seem to be a tension between the TCC and a landscape picture.

Chapter 8

Quintessence in a Landscape

First, we recall some basic facts about quintessence. The equation of state $p = w\rho$ leads to evolution of the scale factor, according to:

$$a(t) = a(t_0)(\frac{t}{t_0})^{\frac{2}{3(1+w)}}. \tag{8.1}$$

For $w = 1$, a free massive field,

$$a(t) \propto t^{1/3}.$$

More generally, this result holds when, in some era, one can neglect the potenital. $w \leq -1/3$ leads to quintessence; $a(t)$ grows faster than $t \sim \frac{1}{H}$.

We will focus on $w < -1/3$, considering a field ϕ with a canonical kinetic term and an exponential potential,

$$V(\phi) = e^{-\lambda\phi} \tag{8.2}$$

in units with reduced Planck mass, $\tilde{M}_p = 1$. For $\lambda < \sqrt{6}$

$$w = -1 + \frac{\lambda^2}{3} \tag{8.3}$$

with $\lambda < \sqrt{2}$ necessary for quintessence[37]. One can quickly check this formula for small λ, noting that in this case the second derivative in the equation for ϕ,

$$\ddot{\phi} + \frac{3}{H}\dot{\phi} + V'(\phi) \tag{8.4}$$

can be neglected. So T_{00} and T_{ij} can be computed simply for the exponential potential.

So now the interesting question is: suppose one has a string model with such a potential and that this accounts for the observed dark energy. In a landscape context, we expect that there are states nearby with negative cosmological constant. We can model this by considering two fields, ϕ and χ, with potential such that $\chi = 0$, $\phi > 0$ corresponds to the quintessence state, and $\chi = \mu,\ \phi = 0$ corresponds to an AdS minimum. The TCC raises the question: what is the lifetime of the quintessence state?

8.1 Tunneling from Quintessence-Like states in Quantum Mechanics

We first consider a quantum mechanical problem, with two degrees of freedom, χ and ϕ, which exhibits tunneling from a time-dependent configuration of the coordinates. In particular, classically there is a lowest energy configuration for some value of $(\chi, \phi) = (\mu, 0)$ and a higher energy configuration, where $\chi = 0$ and ϕ is not uniquely fixed, but instead the potential falls to zero for large ϕ and $\chi = 0$:

$$V(\chi, \phi) = \lambda\phi^2(\chi)^2 + \Gamma(\chi^2 - \mu^2)^2 + \delta\frac{(\chi - \mu)^2}{\phi^2 + \mu^2} \tag{8.5}$$

This has a global minimum at $\chi = \mu$, $\phi = 0$, $V = 0$. At $\chi = 0$, it has runaway behavior for ϕ.

The false "minimum" has $\chi = 0$, ϕ rolling, with

$$V(\phi) = \delta \frac{\mu^2}{\phi^2 + \mu^2} \tag{8.6}$$

(Note we are assuming here that $\delta < \mu^4$; other parameters have been chosen for simplicity; small changes will not alter the behavior of the potential).

This model suggests focusing on a single degree of freedom, x, with:

$$V(x) = -V_0 \quad x < x_0 \qquad V(x) = \frac{\delta}{x^2} \; x >> x_0 \tag{8.7}$$

We are interested in tunneling from a configuration described by a wave packet centered at $x > x_0$, and evolving with time. If the wave packet is Gaussian, and sufficiently narrow, there will be a huge suppression of the wave function in the region $x < x_0$. The question is: what is the natural value for this width, and how does the width grow with time.

It is worth recalling some facts familiar from elementary quantum mechanics.

1. Wave packet evolution for a free particle: consider a system described at $t = 0$ by a Gaussian wave packet with width Δx,

$$\psi(x, 0) = e^{ik_0 x} e^{-\frac{(x - x_{cl})^2}{(\Delta x)^2}}. \tag{8.8}$$

A standard approach to this problem is to Fourier transform, use the known behavior of plane waves, and Fourier transform back. In this case, one obtains:

$$\psi(x, t) = e^{ik_0 x - i\frac{k_0^2}{2m}t} e^{-\frac{(x - x_{cl}(t))^2}{(\Delta x)^2 + i\frac{t}{m}}} \quad x_{cl}(t) = x_0 + \frac{k_0}{m}t \tag{8.9}$$

So the width of the wave packet grows with time according to:

$$(\Delta x(t))^4 = (\Delta x)^4 + \frac{t^2}{m^2} \tag{8.10}$$

This is what one expects from a simple-minded semiclassical argument. With the passage of time, the width of the packet grows as $(\Delta v)t = \frac{\Delta k}{m}t$, giving

$$(\Delta x(t))^2 = (\Delta x)^2 + \frac{(\Delta k)^2 t^2}{m^2} \tag{8.11}$$

or

$$(\Delta x(t)^4) = (\Delta x)^4 + 2\frac{t^2}{m^2} + O(t^4). \tag{8.12}$$

From equation 8.10, we have, at large times,

$$\Delta x(t) = \sqrt{\frac{t}{m}}, \tag{8.13}$$

independent of the initial width of the packet. The width grows much more slowly than the packet moves, i.e.

$$\frac{d\Delta x(t)}{dt} \ll v. \tag{8.14}$$

2. Wave packet evolution for a harmonic oscillator: here, the standard textbook result is that the center of the wave packet evolves classically, and the wave packet does not spread in time. We can see this directly in coordinate space. With

$$\psi(x,t) = e^{-i\frac{k_0^2}{2m}t} e^{-\frac{(x-x(t))^2}{(\Delta x)^2}} \quad x(t) = A\cos(\omega t). \tag{8.15}$$

In the Schrodinger equation, we can compare the term $-\frac{1}{2m}\frac{\partial^2\psi}{\partial x^2}$ with the Kx^2 term. This fixes $(\Delta x)^2 = \frac{1}{\omega^2}$. The wave packet does not spread.

3. Our problem is presumably somewhere in between, behaving nearly like a free particle, with the wave packet spreading, perhaps somewhat more slowly than that for a free particle, particularly in the region where the potential is growing.

$$A \propto e^{\frac{-x(t)^2}{\Delta x^2}} \tag{8.16}$$

If this is the case, for large times, we have a huge suppression of the tunneling amplitude, Rather than a rate of decay per unit time, the rate falls exponentially to zero at large times; one has simply a finite probability to remain in the rolling condition forever.

8.2 Tunneling from Quintessence-Like states in Field Theory (Without Gravity)

For the analogous problem in field theory, we consider two fields, χ and ϕ, with the potential of equation 8.5

$$V(\chi, \phi) = \lambda\phi^2(\chi)^2 + \Gamma(\chi^2 - \mu^2)^2 + \delta\frac{(\chi - \mu)^2}{\phi^2 + \mu^2} \tag{8.17}$$

Again, we have an isolated vacuum at $\phi = 0, \chi = \mu$, and a quintessence-like configuration at $\chi = 0$. For $\phi > \mu$, the χ potential gets steeper and steeper for larger ϕ. Since our interest is in estimating the decay from the region of large ϕ, it makes sense to model the system integrating out χ and writing

$$V_{model}(\phi) = -V_0 \quad \phi < \mu; \quad V(\phi) = \frac{\delta}{\phi^2} \quad \phi > \mu. \tag{8.18}$$

We want to investigate, again, the decay of the quintessence-like state to the isolated vacuum (we can smooth out V_{model} around $\phi = \mu$, if desired).

In terms of the model potential, we can describe the initial bubble corresponding to decay of the system, if we treat $\phi(t)$ as fixed, and take an even more drastic simplification of the potential:

$$V_{simplified}(\phi) = -V_0 \quad \phi < \mu; \quad V(\phi) = 0 \quad \phi > \mu. \tag{8.19}$$

Now we might expect the critical bubble, on dimensional or simple scaling grounds, to have radius:

$$R^2 = \phi(t)^2/V_0. \tag{8.20}$$

Specifically, the kinetic energy term would be of order $\phi(t)^2 R$, while the potential energy term would be of order $R^3 V_0$; the balance determines R. Since the field, ϕ, is free mostly everywhere, we might expect it to have a Gaussian wave functional,

$$\Psi(\phi) = e^{-\int d^3x \phi(x)(\nabla^2)\phi(x)} \tag{8.21}$$

and correspondingly the amplitude to find such a bubble would behave as

$$A \sim e^{-\phi^2 R^2} \sim e^{-\phi^4/V_0}. \tag{8.22}$$

This is, of course, extremely suppressed at large ϕ.

We can obtain the estimate of equation 8.22 by a WKB analysis as in the thin wall case. If we think of a "standard bubble" with size of order R and variations of ϕ on scales of order R, and $\phi \approx \phi_0$ inside the bubble, the lagrangian for R is now:

$$L = \phi_0^2 R\dot{R}^2 + V_0 R^3 - \phi_0^2 R. \tag{8.23}$$

The critical point in the potential is then

$$R^2 = V_0^{-1}\phi_0^2 \tag{8.24}$$

so the WKB estimate yields

$$B \sim \int dR R^{1/2} \sqrt{V_0 R^3} \sim \frac{\phi_0^4}{V_0} \tag{8.25}$$

as above.

8.3 Including Gravity and Checking the TCC Citerion

Without gravity, for large ϕ_0, we have seen that the amplitude for bounce production is enormously suppressed at large ϕ. Here we ask the extent to which gravity might qualitatively alter these results.

8.3.1 The Size of Gravitational Corrections

It is worth considering, first, the size of such corrections in the famliar case of thin wall tunneling[30], for small gravitational coupling, G_N, and with energy splitting ϵ and critical bubble radius R. For the case of decay from flat space to de Sitter space, the energy of the bubble is of order ϵR^3, and the gravitational field is of order $G_N \epsilon R^2$. So the corrections to the action for R are of order $G_N \epsilon^2 R^5$, consistent with equation 3.19 of ref. [31]. These effects grow as ϵ becomes smaller, for fixed G_N, and can be quite dramatic, as stressed by Coleman and Deluccia. For the field theory systems described in the last section, this can also be true for very large $\phi(t)$, but there is a period where these corrections are under control and small. In this period the tunneling amplitude is extremely tiny.

It is in the presence of gravity that we can can actually discuss quintessence,

restricting the term to systems of time-dependent fields with $w < -1/3$. The model of the previous section does not satisfy this criterion. Instead, in considering the TCC and quintessence, we focus on models with exponential potentials yielding suitable w. For this and other systems which truly exhibit quintessence, precise statements require understanding of aspects of quantum gravity, but, if anything, tunneling rates are likely further suppressed.

Indeed, from the work of Coleman and DeLuccia[30], it is known in the thin wall case that inclusion of gravitation further suppresses tunneling, and that there is no semiclassical tunneling if the radius of the would-be anti-deSitter universe is smaller than the would-be bubble size in the absence of gravity. In the absence of gravity, we argued for the models of the previous section that the bubbles would be quite large, of order $\phi_0/\sqrt{V_0}$, while the tunneling amplitude is of order $e^{-\phi_0^4/V_0}$ Gravitational effects may not be within our control, but this estimate is likely to provide some guidance as to tunneling rate. For quintessence, in particular, the kinetic and potential terms in the action are of comparable importance, so we might expect that neglect of the potential term would yield an ($O(1)$ correction to the (large) exponential factor We need to ask: How large is ϕ_0?

8.3.2 How large is ϕ_0?

The value of the field, ϕ_0, at any given time, will control the tunneling amplitude. It is of interest to ask how large ϕ_0 would be if the *present* universe is described by quintessence. Again,without good control of the quantum theory, this may be a hard

question to answer. But the exponential potential is instructive, and strongly suggests that the tunneling amplitude is *extremely* suppressed if quintessence describes the observed dark energy. Note that in a landscape picture of quintessence, such states would have to be quite common, so the sort of estimates we are making here would be fairly typical.

So consider a field, ϕ, with a nearly canonical kinetic terms and potential

$$V = \Lambda^4 e^{-\lambda\phi} \tag{8.26}$$

If Λ = TeV, say, then $\lambda\phi \sim \log(10^{59})$ to describe the current dark energy. We know that λ can't be too large for quintessence, probably not larger than $\frac{1}{\sqrt{3}}$ so ϕ has to be something like 200 in Planck units (note that if Λ is larger than TeV scales, as one might expect, ϕ_0 is larger still). So ϕ_0^4/V_0 which is the action of the critical bubble without gravity, is potentially huge. E.g. if $V_0 \sim M_p^4$, then the bubble is huge, as is the bounce action. The would-be initial bubble itself is two orders of magnitude larger than the AdS radius, suggestive, following [30] that the tunneling amplitude may vanish altogether.

We cannot make completely reliable statement for the strongly coupled system we are considering, but we would be surprised if the gravitational result were wildly different from the result neglecting general relativity. Indeed, because of the large size of the critical bubble in the semiclassical treatment, as we have said, we think it likely that the tunneling amplitude simply vanishes for ϕ_0 sufficiently large, and in particular for ϕ_0 as large as required to account for the presently observed dark energy.

Chapter 9

Discussion and Conclusions

Our results suggest a conflict between the TCC and conventional (albeit highly speculative) conjectures about the string landscape. If we abandon the de Sitter Swampland Conjecture, than the TCC provides a significant constraint on possible metstable de Sitter states. While little is known about such would-be states (though there are plausible conjectures, for example [6], it would seem to rule out, for example, states with positive cosmological constant and even *very* approximate supersymmetry[38]. If we hold to the conjecture, so that the observed dark energy is a form of quintessence, than these states are extremely long lived once the field has evolved to a region with very small cosmological constant. This follows if, as one might expect, there are some modest number of negative cosmological constant states accessible to the system. validity of the TCC implies this quintessence state must be surrounded by some sort of dense set of AdS minima, or we have to be extremely lucky that it there is a well placed such state nearby.

There is another possible way out. If the parameter Λ in equation 8.26 is *extremely* small, one might avoid the necessity for large ϕ. This would imply a tuning conition comparable to the usual one for the cosmological constant. It is not clear to us whether this might have a straightforward anthropic explanation. We leave to the reader the question of how plausible this might seem.

It appears most likely that either the landscape picture does not hold, or that the TCC is not valid and the theory somehow escapes the puzzles associated with the growth of subplanckian fluctuations to horizon size.

Part III

Dark Matter as Remnants of Evaporation of Primordial Black Holes

Chapter 10

Introduction

The nature of non-baryonic dark matter and the origin of the matter-antimatter asymmetry in the universe are two of the most pressing questions at the junction of particle physics and cosmology (see e.g. [39, 40]). The direct detection of gravitational waves [41] has triggered renewed interest in the role black holes might play in connection with these two outstanding open questions (see e.g. [42–44] and references therein).

The idea that black hole evaporation can lead to the production of particles in the early universe and possibly to the generation of a baryon asymmetry or of dark matter has a rather long history. In fact, it dates back to early work by Hawking [45] and Zel'dovich [46], and to subsequent work by Carr [47], where it was pointed out that evaporation might produce a baryon asymmetry because of intrinsic CP-violating effects, or because of accidental statistical excesses. Subsequent work invoked GUT-scale physics, which generically violates CP and baryon number, as a culprit for the generation of the matter-antimatter asymmetry, and specifically CP- and B-violating

decays of GUT-scale particles produced in PBH evaporation. This was first (to our knowledge) envisioned in Ref. [48], and further elaborated upon in Ref. [49–51].

More recently, studies have considered the possibility that primordial black holes be responsible for both the generation of a baryon asymmetry *and* of the dark matter. Specifically, Ref. [52] considers the concurrent generation of a baryon asymmetry from GUT boson decays in inflationary and in ekpyrotic/cyclic models, and the possible presence of dark matter in the form of Planck-scale relics from the evaporation of light primordial holes. The key assumption in Ref. [52] is that the black holes dominate the universe's energy budget by the time they decay. More recently, Ref. [53] dealt with the possibility of a generation of the matter asymmetry from asymmetric sterile neutrino decays, through leptogenesis, and the co-genesis of dark matter from Hawking evaporation. Here, the assumption is, again, that the energy density of the universe is dominated by the primordial black holes before they evaporate. Ref. [53] additionally allows for a possible entropy injection episode *after* the evaporation of the primordial holes. Ref. [54] and [55] recently focused on production of dark matter from black hole evaporation (the second specifically WIMP dark matter), while Ref. [56] and [57] considered scenarios technically similar to asymmetric dark matter production from black hole evaporation that we also entertain below, although the first study in the context of mirror matter and the second in the context of asymmetric Hawking radiation.

In the present study, we are not concerned with *how* primordial black holes were produced following inflation (any pre-existing population would be presumably inflated away). The conditions under which a cosmologically relevant population of

primordial black holes are produced have been known for a long time, ever since the seminal work of Zel'dovich and Novikov from over a half century ago [58]. We will not review them here. In fact, in what follows we will use the relative abundance of primordial black holes at formation as a free parameter.

We intend to study here the generic possibility that primordial black hole evaporation at very early times (much earlier than, say, the epoch when the synthesis of light elements occurs) plays a key role in the genesis of dark matter and/or the baryon asymmetry in the universe. We will be agnostic about the fate of black holes as their mass approaches the Planck scale, and consider both complete evaporation, and the possibility that evaporation stops around or below that scale, leaving Planck-scale relics. We consider a variety of scenarios for the genesis of the matter-antimatter asymmetry, including GUT-scale baryogenesis, leptogenesis, and asymmetric co-genesis of dark and ordinary matter. Finally, we discuss possible tell-tale signals of this general framework.

The structure of this manuscript is as follows: in the following section 11 we outline our framework; sec. 12.1 and 12.2, respectively, discuss the generation of dark matter and of a baryon asymmetry from primordial black hole evaporation, after a general discussion of particle production from hole evaporation; sec. 13 presents our results and a discussion thereof, and the final sec. 14 concludes.

Chapter 11

Outline of the framework

In this study, we explore the possibility that primordial black hole evaporation produced both the dark matter and the baryon asymmetry. We entertain the possibility that the dark matter be a species χ, with mass m_χ belonging to a *dark sector* with a number of degrees of freedom g_χ that ranges, for definiteness, from 1 to 100. We do not make any assumption on the details of the dark sector spectrum. In principle, these details affect the temperature dependence of the number of degrees of freedom in the early universe; however, as we show below, the quantities relevant for us all depend quite weakly on that. We therefore neglect details of the dark sector spectrum and its impact on the number of degrees of freedom as a function of temperature, and assume the dark sector is all degenerate at the same mass scale m_χ.

We assume that the χ never attains thermal equilibrium after being produced (unless we specify otherwise, as is the case when we discuss the case of asymmetric dark matter), and that no processes exist that can *freeze in* any significant abundance

of χ after black hole evaporation [59]. We also entertain both the possibility that black hole evaporation stops at a black hole mass $fM_{\rm Pl}$, with $M_{\rm Pl}$ the reduced Planck mass, leading to a multi-component dark matter scenario consisting of the species χ produced by evaporation and of the Planck-scale relics, and the second possibility that evaporation leads to the complete disappearance of the primordial holes ($f = 0$) and thus to a single-dark matter scenario.

As far as the production of the baryon asymmetry, we entertain three distinct possibilities:

1. That the baryon asymmetry is produced by the B-, L-, and CP-violating decays of a GUT boson X of mass $10^{15} \lesssim m_X/\text{GeV} \lesssim 10^{17}$;

2. That the baryon asymmetry stems from leptogenesis induced by the CP violating decays of heavy right-handed neutrinos with masses at the scale M_ν;

3. That both the baryon asymmetry and the dark matter are produced by the decay of heavy right-handed neutrinos (or some other massive species) into both dark matter/dark sector fields and standard model/visible sector fields, with the dark matter produced by evaporation annihilating away.

Unlike in previous studies, here we let the initial abundance β of primordial black holes at the epoch of formation, at a time t_i normalized to the radiation density,

$$\beta \equiv \frac{\rho_{\rm PBH}(t_i)}{\rho_{\rm rad}(t_i)}, \tag{11.1}$$

to be a free parameter.

As mentioned above, we do consider the possibility that relics of mass $fM_{\rm Pl}$ are left over from PBH evaporation. In this case the approximate constraint is [60]

$$\beta(M_{\rm PBH}) \lesssim 2.8 \times 10^{-28}\ f^{-1} \left(\frac{M_{\rm PBH}}{M_{\rm Pl}}\right)^{3/2}. \tag{11.2}$$

We assume for simplicity that the mass function of primordial black holes (PBH) is monochromatic and centered at a mass $M_{\rm PBH}$ (see e.g. [61] for a motivation to this assumption, and [62] for a recent study of the optimal mass function for dark matter in the form of PBH). The range of viable black hole masses is constrained from below by the requirement that the black holes form when the Hubble rate is at or below the Hubble rate during inflation H_*. The latter is constrained by Planck observations [63] to be

$$\frac{H_*}{M_{\rm Pl}} < 2.7 \times 10^{-5} \quad (95\%\ \text{C.L.}). \tag{11.3}$$

If, as we assume here, primordial black holes form during the radiation domination epoch, their initial mass is

$$M_{\rm PBH} = \gamma \frac{4\pi}{3} \rho H^{-3}, \tag{11.4}$$

where $\gamma \sim 0.2$ [64], and the Planck limit translates to

$$\frac{M_{\rm PBH}}{M_{\rm Pl}} > \frac{4\pi\gamma}{2.7 \times 10^{-5}} \simeq 9.1 \times 10^4 \quad (95\%\ \text{C.L.}). \tag{11.5}$$

Notice that the density of PBHs depends on the spectrum of primordial density perturbations $\delta \equiv \delta\rho/\rho$, which at a given epoch has a certain probability distribution $P(\delta)$, for instance of Gaussian form; the fraction of energy density of the universe that

Mass (g)	T_H (GeV)	τ (s)	$T_{\rm evap} = T(\tau)$ (GeV)
$5M_P \simeq 10^{-4}$	1.7×10^{17}	10^{-41}	2×10^{17}
1	1.7×10^{13}	4×10^{-29}	2×10^{11}
10^3	1.7×10^{10}	4×10^{-20}	6×10^6
10^6	1.7×10^7	4×10^{-11}	200
10^9	1.7×10^4	0.04	0.006
10^{12}	17	$4 \times 10^7 \sim 1$ yr	~ 1 keV

Table 11.1: Mass, Hawking-Gibbons temperature, lifetime, and temperature corresponding to the evaporation time for a few illustrative black hole masses.

collapses to PBHs is then

$$\beta(M_{\rm PBH}) = \int_{\delta_c}^{\infty} P(\delta) d\delta,$$

with $\delta_c \sim \gamma$ the critical overdensity; in the case of Gaussian density perturbations with mass variance σ at horizon crossing, $\beta \sim \exp(\delta_c^2/(2\sigma^2)$; since generally $\delta_c \gg \sigma$, only a small fraction of the energy density of the universe thus collapses to form PBHs, explaining why $\beta \ll 1$.

The upper limit to the mass of the PBH, in our framework, derives from the requirement that evaporation happens well before Big Bang Nucleosynthesis. In principle this is not a hard requirement, but, should it not be satisfied, the resulting limits on $\beta(M_{\rm PBH})$ would rule out any significant production of either dark matter or the baryon asymmetry from PBH evaporation, defeating the point of our study.

We now quickly summarize PBH evaporation: upon integrating the mass loss rate of PBH from Hawking-Gibbons evaporation from a black body at temperature $T_H \equiv M_{\rm Pl}^2/M_{\rm PBH}$, and neglecting grey-body factors [65], the lifetime of a PBH of mass $M_{\rm PBH}$ is

$$\tau = \frac{160}{\pi g} \frac{M_{\rm PBH}^3}{M_{\rm Pl}^4}, \tag{11.6}$$

where g are the number of degrees of freedom of the radiated particles (including the 7/8 factor for fermions), which, here, are all particles with mass smaller than T_H. The radiation bath temperature corresponding to the time τ is calculated in the standard way for a radiation-dominated cosmology, assuming instantaneous thermalization of the evaporation products: using Friedmann's equation [53]

$$\frac{\pi^2}{30} g_* T_{\rm evap}^4 = 3 M_{\rm Pl}^2 H_{\rm evap}^2 \simeq 3 M_{\rm Pl}^2 \tau^{-2} \tag{11.7}$$

with g_* the number of effective relativistic degrees of freedom, we get

$$\frac{T_{\rm evap}}{M_{\rm Pl}} \simeq 0.77 \left(\frac{g_*}{100}\right)^{-1/4} \left(\frac{g}{100}\right)^{1/2} \left(\frac{M_{\rm Pl}}{M_{\rm PBH}}\right)^{3/2}, \tag{11.8}$$

which is of course only valid if evaporation ends during radiation domination, which is always the case for us.

We list in Table 11.1 masses, Hawking-Gibbons temperatures, lifetimes, and temperature corresponding to the evaporation time for a few illustrative black hole masses. The table shows that in order to avoid impacting the synthesis of light elements (at times of $t \sim \mathcal{O}(1$ sec), the PBH under consideration here are required to be lighter than approximately 1,000 t, i.e. 10^9 grams.

Chapter 12

Particle production from Primordial Black Hole Evaporation

We intend to calculate the abundance of right-handed neutrinos or dark matter (generically, of any massive particle X) produced by the evaporation of PBH in an adiabatically expanding universe, if the relative density of PBH to radiation at PBH formation time t_i is $\beta(t_i) = \rho_{\rm PBH}/\rho_{\rm rad}$. Indicating with N_X the number of particles X produced in the evaporation of one single hole, the number-to-entropy density of particles X at the present epoch is

$$\frac{n_X}{s}(t_{\rm now}) = N_X \frac{n_{\rm PBH}}{s}(t_i) = N_X Y_i. \tag{12.1}$$

To calculate Y_i, we use the definition of β,

$$\beta = M_{\rm PBH}\frac{n_{\rm PBH}(t_i)}{\rho_{\rm rad}(t_i)} = M_{\rm PBH}\frac{s(t_i)}{\rho_{\rm rad}(t_i)}Y_i = \frac{4}{3}\frac{M_{\rm PBH}}{T_i}Y_i \tag{12.2}$$

where in the last equality we have assumed that at very large temperatures $g \simeq g_*$, the latter indicating the entropic degrees of freedom. From Eq. (11.4) we then get

$$\frac{T_i}{M_{\rm Pl}} \simeq 0.87 \left(\frac{M_{\rm Pl}}{M_{\rm PBH}}\right)^{1/2} \left(\frac{g_*}{100}\right)^{-1/4}. \tag{12.3}$$

Now, substituting Eq. (12.3) into Eq. (12.2) and the expression for Y_i,

$$Y_i = 0.65\ \beta\ \left(\frac{g_*}{100}\right)^{-1/4} \left(\frac{M_{\rm Pl}}{M_{\rm PBH}}\right)^{3/2}, \tag{12.4}$$

into Eq. (12.1), we get

$$\frac{n_X}{s}(t_{\rm now})\ \simeq\ 0.65\ \beta\ N_X \left(\frac{g_*}{100}\right)^{-1/4} \left(\frac{M_{\rm Pl}}{M_{\rm PBH}}\right)^{3/2}. \tag{12.5}$$

The calculation of N_X follows Ref. [52]. Assume that $M_X < T_H = M_{\rm Pl}^2/M_{\rm PBH}$, and assume that evaporation does not stop at $M_{\rm Pl}$, i.e. $f = 0$. In this case,

$$N_X \simeq \frac{g_X}{g} \int_{M_{\rm PBH}}^{0} \frac{-dM}{3T} = \frac{g_X}{g} \int_{T_H}^{\infty} \frac{M_{\rm Pl}^2}{3T^3} dT = \frac{g_X}{6g} \left(\frac{M_{\rm PBH}}{M_{\rm Pl}}\right)^2. \tag{12.6}$$

In the first equality, we assumed that the number of radiated particle is given by the ratio of the radiation energy from PBH evaporation, $-dM$, divided by the mean energy of a black-body of temperature T, $\langle E \rangle_T \simeq 3T$ (we notice that this is an approximate result that assumes the particles produced at evaporation to be spin zero, as well as a trivial, constant absorption cross section; in more realistic setups, there is a complicated dependence of the factor in front of T on the spectrum and spin of the particles the PBH evaporates to, see e.g. the classical literature on this point, Ref. [65–67]).

The ratio of the degrees of freedom g_X/g, where $g = g_X + g_{\rm SM}$, the latter $g_{\rm SM}$ indicating the "standard model" degrees of freedom, corresponds to the approximate

ratio of emitted X particles, neglecting the effects of charge and spin on the evaporation rate, and in the second equality we used the relation between Hawking-Gibbons temperature and black hole mass. In the case where evaporation stops when the black hole mass is equal to $fM_{\rm Pl}$, the equation above is modified as follows:

$$N_X^f \simeq \frac{g_X}{6g}\left(\left(\frac{M_{\rm PBH}}{M_{\rm Pl}}\right)^2 - f^2\right), \tag{12.7}$$

and of course reduces to the result above if $M_{\rm PBH} \gg fM_{\rm Pl}$; given the constraint in Eq. (11.5) above, unless $f \gtrsim 10^4$, a range theoretically unmotivated for evaporation to stop, Eq. (12.6) above is perfectly adequate, and we shall use it from now on.

Notice that in principle massive particles X can be produced by PBH evaporation even if the *initial* Hawking-Gibbons temperature is *lower* than m_X. In that case, X production proceeds from the moment when $t_H = M_X$, thus

$$N_X \simeq \frac{g_X}{g}\int_{M_X}^{\infty}\frac{M_{\rm Pl}^2}{3T^3}dT = \frac{g_X}{6g}\left(\frac{M_X}{M_{\rm Pl}}\right)^{-2}. \tag{12.8}$$

In summary, given a sector with g_X degrees of freedom and a stable relic X of mass M_X, the cosmological abundance $\Omega_X = \rho_X/\rho_c$, with ρ_c the critical energy density of the universe, is

$$\begin{aligned}
\Omega_X &= \frac{M_X}{\rho_c}\frac{n_X}{s}(t_{\rm now})s_{\rm now} = \frac{M_X}{\rho_c}N_X Y_i s_{\rm now} \qquad (12.9)\\
&\simeq 0.11\ \beta\ \frac{M_X s_{\rm now}}{\rho_c}\left(\frac{g_*}{100}\right)^{-1/4}\left(\frac{g_X}{g}\right)\left(\frac{M_{\rm PBH}}{M_{\rm Pl}}\right)^{1/2}, \qquad M_X < M_{\rm Pl}^2/M_{\rm PBH},\\
&\simeq 0.11\ \beta\ \frac{M_X s_{\rm now}}{\rho_c}\left(\frac{g_*}{100}\right)^{-1/4}\left(\frac{g_X}{g}\right)\left(\frac{M_{\rm Pl}^7}{M_{\rm PBH}^3 M_X^4}\right)^{1/2}, \qquad M_X > M_{\rm Pl}^2/M_{\rm PBH}.
\end{aligned}$$

Since [68]

$$\rho_c = 1.0537\times 10^{-5}\ h^2\ \frac{\rm GeV}{\rm cm^3} \simeq 4.78\times 10^{-6}\left(\frac{h}{67.37}\right)^2\ \frac{\rm GeV}{\rm cm^3} \tag{12.10}$$

and [68]

$$s_{\rm now} = 2,891.2 \left(\frac{T_{\rm CMB}}{2.7255}\right)^2 \ {\rm cm}^{-3}, \tag{12.11}$$

we can recast the equations above, for $g_* = 106.75 + 1$ (which assumes $g_{\rm DM} = 1$ for definiteness), as

$$\begin{aligned} \Omega_X &\simeq 6.5 \times 10^7 \ \beta \left(\frac{M_X}{\rm GeV}\right) \left(\frac{g_X}{g}\right) \left(\frac{M_{\rm PBH}}{M_{\rm Pl}}\right)^{1/2}, \qquad M_X < M_{\rm Pl}^2/M_{\rm PBH}, \\ &\simeq 6.5 \times 10^7 \ \beta \left(\frac{M_X}{\rm GeV}\right) \left(\frac{g_X}{g}\right) \left(\frac{M_{\rm Pl}^7}{M_{\rm PBH}^3 M_X^4}\right)^{1/2}, \qquad M_X > M_{\rm Pl}^2/M_{\rm PBH}. \end{aligned} \tag{12.12}$$

Since the radiation energy density redshifts like a^{-4}, with a the scale factor, while pressure-less matter redshifts as a^{-3}, for sufficiently large β, the universe could become matter-dominated by PBH prior to evaporation. This condition can be expressed as

$$\beta_f = \frac{\rho_{\rm PBH}(T_{\rm evap})}{\rho_{\rm rad}(T_{\rm evap})} > 1. \tag{12.13}$$

Assuming entropy conservation, we can relate the initial value of β to β_f in the equation above,

$$\beta_f = \beta \frac{T_i}{T_{\rm evap}} \simeq 1.1 \left(\frac{g}{100}\right)^{-1/2} \left(\frac{M_{\rm PBH}}{M_{\rm Pl}}\right), \tag{12.14}$$

where we used Eq. (12.3) and (11.8) to express T_i and $T_{\rm evap}$ as functions of $M_{\rm PBH}$. If PBH get to dominate the energy density of the universe prior to evaporation, the number density of particles produced by evaporation ceases to depend on β, as pointed out by Ref. [53], as a result of the balance between the dilution of the number density of particles produced by evaporation and of the additional particles resulting from $\beta_f > 1$. In all our results, we highlight the parameter space on the $(M_{\rm PBH}, \beta)$ plane where $\beta_f = 1$

(for $g_\chi = 1$ plus Standard Model degrees of freedom) with a thick purple line; for β values above that line, our results are β-independent.

12.1 Dark Matter from PBH evaporation

We consider three mechanisms for dark matter production from PBH evaporation: direct production from evaporation, Planck-scale relics from evaporation, and asymmetric dark matter production. We postpone the discussion of the latter to the next section, and Eq.(12.9) directly gives the abundance of dark matter from PBH evaporation.

If evaporation stops at a mass scale $fM_{\rm Pl}$, the cosmological abundance of Planck-scale relics, $\Omega_P = (fM_{\rm Pl} n_{\rm PBH}(t_{\rm now}))/\rho_c$ is given by

$$\begin{aligned} \Omega_P &= \frac{fM_{\rm Pl}}{\rho_c} Y_i s_{\rm now} = 0.65\ \beta\ f\ \frac{M_{\rm Pl} s_{\rm now}}{\rho_c} \left(\frac{g_*}{100}\right)^{-1/4} \left(\frac{M_{\rm Pl}}{M_{\rm PBH}}\right)^{3/2}, \\ &\simeq 9.4 \times 10^{26}\ \beta\ f\ \left(\frac{M_{\rm Pl}}{M_{\rm PBH}}\right)^{3/2}, \end{aligned} \tag{12.15}$$

again with $g_* = 106.75 + 1$ in the second equation.

Requiring that the dark matter in the universe have a density $\Omega_{\rm CDM} \simeq 0.21$ [68] forces a condition across the model parameters g_χ, m_χ, $M_{\rm PBH}$, f and β (where we indicated with χ the dark matter from PBH evaporation) such that

$$\Omega_{\rm CDM} = \Omega_\chi(g_\chi, m_\chi, M_{\rm PBH}, \beta) + \Omega_P(f, M_{\rm PBH}, \beta). \tag{12.16}$$

Also, wherever $\Omega_P, \Omega_\chi > \Omega_{\rm CDM}$, the corresponding region of parameter space is excluded as too much dark matter is produced by either evaporation or Planck-scale leftover relics,

or both (of course, this assumes no episode of entropy injection that would dilute the relics' density, see e.g. [53]). Notice that regions with *underabundant* dark matter from either Planck relics or evaporation are not ruled out, since some other dark matter component might provide the remaining part of the observed cosmological dark matter density.

An important constraint on dark matter χ produced from PBH evaporation comes from the requirement that the dark matter be *cold enough* as to avoid disruption of small-scale structures via free-streaming. We follow here the discussion in Ref. [53]: The initial average energy of particles from the evaporation of a hole of mass $M_{\rm PBH}$ is $6T_H = 6M_{\rm Pl}^2/M_{\rm PBH}$ (see the derivation below in Eq. (12.19)). Because we assume the dark matter particles are never in kinetic or chemical equilibrium, the particle momentum today is simply the redshifted value of the momentum at production,

$$p_{\rm now} = \frac{a_{\rm evap}}{a_{\rm now}} p_{\rm evap}, \tag{12.17}$$

where $a_{\rm now} = 1$. The energy of the dark matter particle at evaporation can be calculated as follows: the average energy of particles radiated by a PBH with a Hawking-Gibbons radiation temperature T_H is $3T_H$ (with the caveats explained above – this is a simplifying approximation!). The total number of particles emitted by the PBH is approximately

$$N = \int_0^N dn = \int_{T_H}^{\infty} \frac{M_{\rm Pl}^2}{3T^3} dT = \frac{1}{6}\left(\frac{M_{\rm Pl}}{T_H}\right)^2. \tag{12.18}$$

The mean energy of the radiated particles is thus

$$\bar{E} \simeq \int_0^N (3T)\frac{dn}{N} = 6\left(\frac{T_H}{M_{\rm Pl}}\right)^2 \int_{T_H}^{\infty} \frac{M_{\rm Pl}^2}{T^2} dT = 6\left(\frac{T_H}{M_{\rm Pl}}\right)^2 \left(\frac{M_{\rm Pl}^2}{T_H}\right) = 6T_H. \tag{12.19}$$

Notice that this average energy is different from the average energy at the beginning of evaporation, since it averages over all temperatures from that initial temperature to infinity. Now, since $m_\chi < T_H$ in order for the dark matter to be produced, $\bar{E} \simeq \bar{p} = p_{\rm evap}$. The last ingredient to calculate the dark matter velocity today is $a_{\rm evap}$. Fixing $a_{\rm now} = 1$, the scale factor at matter-radiation equality $a_{\rm eq} = \Omega_r/\Omega_m$. Then, using Friedman's equation, and the fact that $\rho \sim a^4$ in radiation domination, we have

$$a_{\rm evap} = a_{\rm eq}\left(\frac{\rho_{\rm eq}}{\rho_{\rm evap}}\right)^{1/4} = a_{\rm eq}\left(\frac{\rho_c/a_{\rm eq}^3}{3M_{\rm Pl}^2/t_{\rm evap}^2}\right)^{1/4} \simeq 7\times 10^{-32}\left(\frac{M_{\rm PBH}}{M_{\rm Pl}}\right)^{3/2} \tag{12.20}$$

where we used Eq. (11.7) in the next-to-last equality. The present velocity of dark matter produced from the evaporation of a PBH of mass $M_{\rm PBH}$ is thus

$$v_\chi = \frac{p_{\rm now}}{m_\chi} \simeq 4\times 10^{-31}\left(\frac{m_\chi}{M_{\rm Pl}}\right)^{-1}\left(\frac{M_{\rm PBH}}{M_{\rm Pl}}\right)^{1/2}. \tag{12.21}$$

Assuming that only redshift contributes to setting the current dark matter velocity, using the constraint of Ref. [69] on the velocity of thermal relics today,

$$v_\chi \lesssim 4.9\times 10^{-7}, \tag{12.22}$$

we have

$$\frac{m_\chi}{1\ {\rm GeV}} \gtrsim 2\times 10^{-6}\left(\frac{M_{\rm PBH}}{M_{\rm Pl}}\right)^{1/2}. \tag{12.23}$$

The constraint above, together with the minimal primordial black hole mass allowed by CMB results, Eq. (11.5), sets the minimal possible dark matter mass, if produced from evaporation,

$$m_\chi \gtrsim 0.6\ {\rm MeV}. \tag{12.24}$$

Notice that the constraint in Eq. (12.24) applies only if a substantial fraction of the dark matter is produced by evaporation from PBH's of mass $M_{\rm PBH}$. Assuming that such fraction is, say, 10% of the dark matter in the universe, given that the maximal density of dark matter from evaporation corresponds to the dark matter dominating the number of degrees of freedom PBH evaporate to, our constraint applies to (for instance for $m_\chi < M_{\rm Pl}^2/M_{\rm PBH}$)

$$\beta \gtrsim 0.1 \frac{\rho_c}{m_\chi s_{\rm now}} \left(\frac{g_*}{100}\right)^{1/4} \left(\frac{g_\chi}{g}\right) \left(\frac{M_{\rm PBH}}{M_{\rm Pl}}\right)^{-1/2}. \tag{12.25}$$

Notice that this is likely a fairly conservative constraint, as the limit in Eq. (12.22) assumes 100% of the dark matter has the quoted velocity.

12.2 Baryon Asymmetry from PBH evaporation

Here, we consider three classes of models for baryogenesis via PBH evaporation: baryogenesis via non-thermal leptogenesis, baryogenesis via the decay of grand unification gauge bosons (GUT baryogenesis) and, finally, we entertain the possibility that the dark matter is produced in conjunction with an asymmetry in the baryon sector.

In all cases, we determine whether PBH evaporation can lead to the observed baryon asymmetry, with a baryon-number-to-entropy density of [68]

$$n_B/s \approx 8.8 \times 10^{-11}.$$

12.2.0.1 Baryogenesis via leptogenesis

In the case of baryogenesis via leptogenesis,

$$\frac{n_B}{s} = N_\nu \, \varepsilon \, \kappa \, Y_i \simeq 0.65 N_\nu \, \varepsilon \, \kappa \, \beta \left(\frac{g_*}{100}\right)^{-1/4} \left(\frac{M_{\rm Pl}}{M_{\rm PBH}}\right)^{3/2}, \tag{12.26}$$

with

$$N_\nu \simeq \frac{g_\nu}{g} \int_{M_{\rm PBH}}^{0} \frac{-dM}{3T} = \frac{g_\nu}{g} \int_{T_0}^{\infty} \frac{M_{\rm Pl}^2}{3T^3} dT = \frac{g_\nu}{6g} \left(\frac{M_{\rm PBH}}{M_{\rm Pl}}\right)^2, \quad M_\nu < T_H = M_{\rm Pl}^2/M_{\rm PBH} \tag{12.27}$$

$$N_\nu \simeq \frac{g_\nu}{g} \int_{M_\nu}^{\infty} \frac{M_{\rm Pl}^2}{3T^3} dT = \frac{g_\nu}{6g} \left(\frac{M_\nu}{M_{\rm Pl}}\right)^{-2}, \quad M_\nu > T_H, \tag{12.28}$$

and where M_ν is the right-handed neutrino mass scale (for simplicity we assume all right-handed neutrinos to be close-to-degenerate in mass), with ε the CP asymmetry factor of the right-handed neutrino decays, and with $\kappa \approx 0.35$ the conversion ratio of leptons to baryons [49]. An important constraint for the baryogenesis-via-leptogenesis scenario is that the inverse-decay of right handed neutrinos be out of equilibrium. This is guaranteed if the temperature of the universe at PBH evaporation is smaller than M_ν, i.e. if

$$M_\nu > T_{\rm evap} \simeq 1.9 \times 10^{18} \text{ GeV} \left(\frac{M_{\rm Pl}}{M_{\rm PBH}}\right)^{3/2}, \tag{12.29}$$

where we assumed $g_* \simeq g \simeq 100$. In the baryogenesis-via-leptogenesis scenario we also require that the evaporation temperature be larger than the electroweak scale, under which sphaleron rates are highly suppressed, thus enforcing

$$T_{\rm evap} \gtrsim 100 \text{ GeV} \Rightarrow M_{\rm PBH} \lesssim 7.1 \times 10^{10} \, M_{\rm Pl} \simeq 1.4 \times 10^6 \text{ grams}. \tag{12.30}$$

In a model-independent way, the parameter ε is *a priori* unconstrained and of $\mathcal{O}(1)$. However, in specific model realizations, ε can be bounded from above. For instance, for type I seesaw models, barring tuned right-handed neutrino Yukawa textures [70, 71], one has [72]

$$\varepsilon < \frac{3 M_\nu m_{\rm max}}{16 \pi v^2} \simeq 240 \left(\frac{M_\nu}{M_{\rm Pl}}\right) \left(\frac{m_{\rm max}}{0.05 \text{ eV}}\right), \tag{12.31}$$

with v the electroweak vacuum expectation value, and $m_{\rm max}$ the mass of the heaviest left-handed neutrino. In light of that and of cosmological constraints on $m_{\rm max}$ [68], and in this specific model context, only for $M_\nu \simeq 10^{14}$ GeV could $\varepsilon \sim \mathcal{O}(1)$, but not for smaller right-handed neutrino masses. However, larger phases are generically possible, see e.g. fig. 4 of Ref. [71]. In what follows we consider a model independent scenario, and in order to show the maximal possible range of viable parameters, we set here $\varepsilon = 0.5$.

Requiring a baryon asymmetry yield matching observations, and assuming $M_\nu > T_H$ and $g_\nu = 6$, we get the following relation between the right-handed neutrino mass scale, the PBH mass and β

$$\beta \simeq \frac{2.3 \times 10^{-9}}{\varepsilon \ \kappa} \left(\frac{M_{\rm Pl}^7}{M_\nu^4 M_{\rm PBH}^3}\right)^{-1/2}. \tag{12.32}$$

12.2.0.2 GUT baryogenesis

In the scenario where baryogenesis originates from the CP and B-number violating decays of a GUT boson X, carrying g_X degrees of freedom, the produced baryon asymmetry depends on the CP violating parameter [52]

$$\gamma \equiv \sum_i \ B_i \ \frac{\Gamma(X \to f_i) - \Gamma(\bar{X} \to \bar{f}_i)}{\Gamma_X}, \tag{12.33}$$

where B_i is the baryon number of the particular final state f_i, and Γ_X the X decay width. The expression for the resulting baryon asymmetry is then simply

$$\frac{n_B}{s} = N_X \ \gamma \ Y_i \simeq 0.65 N_X \ \gamma\beta \ \left(\frac{g_*}{100}\right)^{-1/4} \left(\frac{M_{\rm Pl}}{M_{\rm PBH}}\right)^{3/2}, \tag{12.34}$$

with, just as above,

$$N_X \simeq \frac{g_X}{6g} \left(\frac{M_{\rm PBH}}{M_{\rm Pl}}\right)^2, \quad M_X < T_H = M_{\rm Pl}^2/M_{\rm PBH} \tag{12.35}$$

$$\simeq \frac{g_X}{6g} \left(\frac{M_X}{M_{\rm Pl}}\right)^{-2}, \quad M_X > T_H, \tag{12.36}$$

We consider a fairly generous range for the mass scale M_X of the GUT gauge bosons X whose decay is responsible for the generation of the baryon asymmetry,

$$10^{15} \lesssim M_X/{\rm GeV} \lesssim 10^{17}; \tag{12.37}$$

a variety of mechanisms can shift the precise energy scale of gauge coupling unficiation, and even when that scale is fixed, M_X is not exactly determined (see e.g. Ref. [73] and references therein). In the plots, we use $g_X = 25$ and $\gamma = 0.1$.

Notice that GUT baryogenesis requires a source of $B - L$ violation to prevent sphaleron washout of the produced baryon asymmetry for models where evaporation happens before the electroweak phase transition, here for masses $M_{\rm PBH} \lesssim 10^6$ g. We postulate in this case the mechanism outlined in Ref. [74], which posits the existence of heavy right-handed neutrinos interacting with the Standard Model Higgs doublet via an effective dimension five operator; as long as the induced lepton-number violating reaction is fast compared to the sphaleron rate (which is generically the case at high enough

temperatures) then the ΔL component of the generated lepton-baryon asymmetry is erased, leaving a net ΔB which is unaffected by sphaleron washout.

12.2.1 Asymmetric Dark Matter

Finally, we consider a simple incarnation of asymmetric dark matter, inspired by the scenario detailed in Ref. [75]. Schematically, the Standard Model is augmented with a dark-sector scalar field ϕ and a Dirac fermion χ coupled to right-handed neutrinos N_i, with Lagrangian density

$$-\mathcal{L} = -\mathcal{L}_{\rm SM} + \frac{1}{2} M_i N_i^2 + Y_{i\alpha} N_i L_\alpha H + \lambda_i N_i \chi \phi + \text{h.c.} \tag{12.38}$$

plus mass terms for the ϕ and χ. χ has lepton number +1, and χ and ϕ are charged under a discrete Z_2 symmetry that ensures the stability of the lightest dark sector state; we assume $m_\chi < m_\phi$, so χ is the stable species[1]. We also need to assume fast, lepton-conserving interactions that thermalize leptons l, the Higgs, and the dark sector fields, annihilating away the symmetric components $l + \bar{l}$ and $\chi + \bar{\chi}$ (including, here, those non-thermally produced by PBH evaporation). Since the symmetric component of the dark matter must annihilate away by hypothesis in this scenario, the dark matter will generically reach kinetic equilibrium , thus reducing its velocity. As a result, the limit in Eq. (12.23) does not apply here.

The N_i decays are CP-violating, and the resulting decay asymmetries are de-

[1]Note that lepton number conservation forces χ to be a Dirac fermion, and to get mass from another fermion $\tilde{\chi}$ with opposite lepton number.

fined summing upon Standard Model generations $\alpha = 1...3$, $\epsilon_L = \sum_\alpha \epsilon_{L_\alpha}$, where

$$\epsilon_\chi = \sum_i \frac{\Gamma(N_i \to \chi\phi) - \Gamma(N_i \to \bar{\chi}\phi^\dagger)}{\Gamma_{N_i}}, \quad \epsilon_L = \sum_i \frac{\Gamma(N_i \to lh) - \Gamma(N_i \to \bar{l}h^\dagger)}{\Gamma_{N_i}}. \quad (12.39)$$

The final asymmetry in each sector does not only depend on the decay asymmetries above, but also by on the details of the models and on washout and transfer effects, which, following Ref. [75], we parameterize with the quantities η_L and η_χ in the two sectors, respectively. Finally, the asymptotic asymmetries must satisfy [76]

$$Y^\infty_{\Delta L} = \epsilon_L \eta_L N_\nu Y_i = \left(\frac{n_B}{s}\right)\frac{37}{12} \simeq 2.7 \times 10^{-10} \quad (12.40)$$

$$Y^\infty_{\Delta \chi} = \epsilon_\chi \eta_\chi N_\nu Y_i \simeq 4.4 \times 10^{-10}\left(\frac{1\ \text{GeV}}{m_\chi}\right), \quad (12.41)$$

where Y_i is the same as what given in Eq. (12.4), N_ν is as given in Eq. (12.27) and, again as above, we assume the N_i to be out of equilibrium and produced from PBH evaporation (thus with a mass satisfying the constraints of Eq. (12.29)).

In the case, for instance, where $M_\nu < T_H$, and thus N_ν is independent of M_ν, we find that

$$N_\nu Y_i \simeq 0.04\beta\left(\frac{M_{\rm PBH}}{M_{\rm Pl}}\right)^{1/2} \quad (12.42)$$

and thus, given a value for $\epsilon_L\eta_L$, there is one value of β that satisfies Eq. (12.40), namely

$$\beta \simeq \frac{6.8 \times 10^{-9}}{\epsilon_L \eta_L}\left(\frac{M_{\rm PBH}}{M_{\rm Pl}}\right)^{-1/2}. \quad (12.43)$$

In turn, given $N_\nu Y_i$ as in Eq. (12.42), there is a one-to-one correspondence between $\epsilon_\chi\eta_\chi$ and m_χ via Eq. (12.41). Specifically,

$$\frac{\epsilon_L\eta_L}{\epsilon_\chi\eta_\chi} \equiv r_{L\chi} \simeq 0.61\left(\frac{m_\chi}{1\ \text{GeV}}\right). \quad (12.44)$$

Chapter 13

Results

We discuss in this section all of our numerical results for the framework described above. Sec. 13.1 assumes complete PBH evaporation and no Planck-scale relics (thus, $f = 0$, where f indicates the mass of PBH relics from evaporation in units of the reduced Planck mass); we show results for both the baryogenesis via leptogenesis (see sec. 12.2.0.1) and for the GUT baryogenesis (sec. 12.2.0.2) scenarios, for a variety of dark matter masses; the following sec. 13.2 assumes $f \neq 0$, and thus the existence of Planck-scale relics contributing to the global cosmological dark matter density, again for both baryogenesis scenarios, and again for a variety of dark matter masses; finally, in sec. 13.2.1 we show results for asymmetric dark matter, for two different values of the right-handed neutrino mass scale.

13.1 Baryogenesis and Dark Matter from (complete) PBH evaporation

As outlined above, we assume exclusive non-thermal dark matter production from PBH evaporation, and we also assume that the dark matter never thermalizes. We intend to address two questions:

(1) What is the range of viable dark matter masses?

(2) Can dark matter and baryogenesis both be accounted for from PBH evaporation? If so, for which PBH masses?

We outlined above general constraints on the dark matter mass: the lower limits stems from Eq. (12.24), while the upper limit corresponds to the maximal mass that can be produced from the evaporation of a PBH of mass $M_{\rm PBH}$; the upper limit lies in the regime where $M_X > T_H = M_{\rm Pl}^2/M_{\rm PBH}$ (for $M_X < T_H$, $M_X < M_{\rm Pl}/(9.1 \times 10^4)$, because of Eq. (11.4)), and is given by the requirement that $N_X > 1$; The maximal possible N_X corresponds to $g_X, g \to \infty$ and thus to $M_X < M_{\rm Pl}/\sqrt{6} \simeq 10^{18}$ GeV.

We present our results in Fig. 13.1. All plots in our study utilize the same parameter space: the $(M_{\rm PBH}, \beta)$ plane (as a reminder, β is the relative energy density of primordial black holes at the time of their genesis). In the plots, we shade in yellow the region at low PBH masses ruled out by the CMB limit of Eq. (11.4) from the lowest possible Hubble rate during inflation; we shade in blue the region excluded by

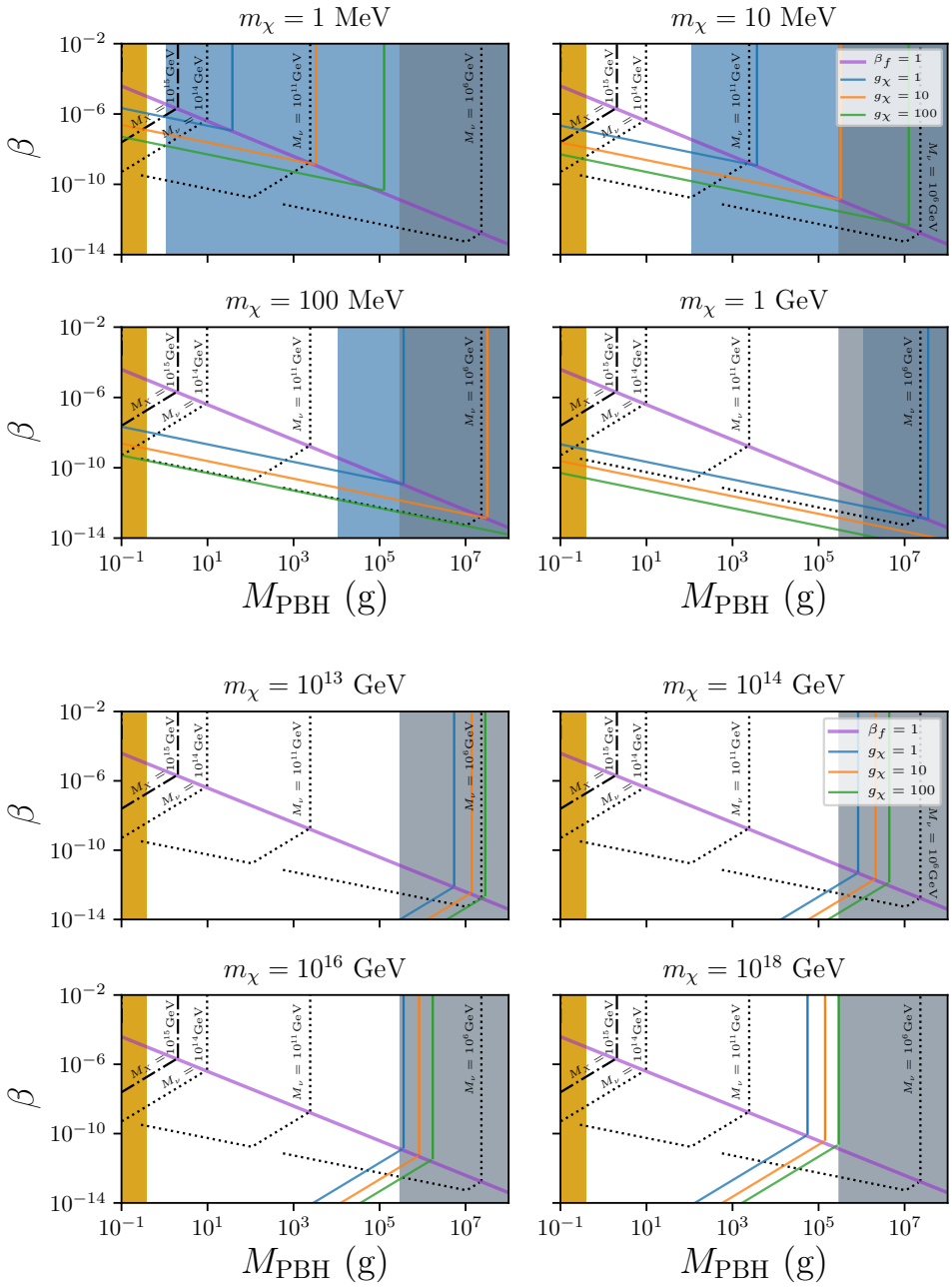

Figure 13.1: Regions of successful production of the observed baryon asymmetry and dark matter on the $(M_{\rm PBH}, \beta)$ plane. The region shaded in yellow on the left is ruled out by the CMB constraint of Eq. (11.5). The blue-shaded region is ruled out by the constraint on the velocity of the dark matter at late times; finally, the grey region violates the constraint of Eq. (12.30), relevant for the leptogenesis scenario. The thick purple line corresponds to $\beta_f = 1$ for $g_\chi = 1$ plus Standard Model degrees of freedom, i.e. for β above that line, PBH eventually dominate the energy density of the universe prior to evaporation. The colored lines correspond to the dark matter mass indicated on top of each panel and varying number of dark-sector degrees of freedom, as indicated in the legend. The dot-dashed lines indicate regions of successful baryogenesis via GUT bosons decay. Finally, the dotted lines indicate regions of successful baryogenesis via leptogenesis, corresponding to different right-handed neutrino mass scales, as indicated, and to a large CP violation parameter $\varepsilon = 0.5$ (smaller CP parameters would shift the curves to proportionally larger values of $\beta \sim 1/\varepsilon$).

the current dark matter velocity limit, Eq. (12.24); finally, we shade in grey the region where PBH evaporation ends below the electroweak scale, and thus baryogenesis via leptogenesis is not effective because of suppressed sphaleron rates, Eq. (12.30).

We indicate with a thick purple line the region where $\beta_f = 1$ for $g_\chi = 1$ plus Standard Model degrees of freedom, i.e. for β above that line, PBH eventually dominate the energy density of the universe prior to evaporation, and particle production becomes β-independent (hence the lines corresponding to successful baryogenesis and dark matter production become vertical).

In the plots, the colorful solid lines correspond to different numbers of dark-sector degrees of freedom: the upper blue line corresponds to $g_\chi = 1$, the orange line to 10 and the green to 100. The dot-dashed line shows the parameter space compatible with GUT baryogenesis for $M_X = 10^{15}$ GeV. Finally, the dotted lines correspond to baryogenesis via leptogenesis with right-handed neutrino mass scales $M_\nu = 10^{14}$ GeV (upper line), $M_\nu = 10^{11}$ GeV (middle line) and $M_\nu = 10^6$ GeV (lower line). We truncate the dotted lines in this plot and in the following plots at PBH masses such that the corresponding non-thermally produced neutrinos would thermalize, thus violating Eq. (12.29). Notice that for intermediate values of M_ν, the envelope giving the lowest possible β for successful leptogenesis is uninterrupted, and that values of $M_\nu < 10^6$ GeV are also possible. Once again, viable leptogenesis occurs in the region encompassed by the dotted lines.

We start with a dark matter mass of 1 MeV in the upper left panel of the top-four plots in figure 13.1. This mass is only slightly above the limit in Eq. (12.24)

(incidentally, we note that slightly lower masses, between 0.6 and 1 MeV, are possible, but correspond to very narrow viable parameter space in $M_{\rm PBH}$). For such light masses, the constraint on the present dark matter velocity, from Eq. (12.22), is quite stringent, and pushes against the constraint on $M_{\rm PBH}$ in Eq. (11.4). Notice that despite the fact that lighter black holes have a larger temperature, the earlier evaporation time means the produced dark matter has more time to cool by redshifting.

Light dark matter particles means, via Eq. (12.9), that larger values of β are needed at a given $M_{\rm PBH}$. In turn, this makes it easier to combine the generation of dark matter from evaporation and of the observed baryon asymmetry. Fig. 13.1 shows that for dark matter masses at around 1 MeV, both leptogenesis and GUT baryogenesis work, with the former suitable for a large number of degrees of freedom, and the latter for a low number of degrees of freedom. PBH dominance of the universe's energy density forces $g_\chi > 1$ in this case. The PBH mass needs to be right around 1 gram for a dark matter of 1 MeV. For sub-MeV dark matter masses we find that the only viable scenario is GUT baryogenesis, for PBH mass slightly below 1 gram, and again $g_\chi \sim 10$.

The upper right plot shows $m_{\rm DM} \sim 10$ MeV. GUT baryogenesis is now no longer possible, while there is substantial overlap with leptogenesis across a fairly extended range of PBH masses from 0.5 to around 100 grams. The same applies to 100 MeV dark matter masses, although here the viable PBH mass range is extended to larger values, up to the limit from the current dark matter velocity, which, for a dark matter mass of 100 MeV, is around a few tens of kg. Finally, for DM masses at the GeV (lower right panel) or more, the parameter space keeps enlarging as the constraint on

the dark matter velocity weakens (for 1 GeV up to ton-scale PBH); leptogenesis remains viable as long as the right-handed neutrino mass is sufficiently low.

In the lower four panels, we show a different regime, where the dark matter mass is very heavy (10^{13} to 10^{18} GeV), and is produced by PBH whose initial temperature is *lower* than the dark matter mass. In this regime, the dependence with $M_{\rm PBH}$ is no longer $\Omega_\chi \sim M_{\rm PBH}^{1/2}$ but is instead $\Omega_\chi \sim M_{\rm PBH}^{-3/2}$ (see Eq.(12.12)). The top two panels illustrate that the dark matter mass must be at least a few $\times 10^{13}$ to be viable, with generally very low right-handed neutrino masses. Notice that the constraint on the PBH mass from evaporation ending prior to the EW phase transition, forces the lowest dark matter mass to be heavier than a few times 10^{12} GeV. Also, notice that GUT baryogenesis is *never* an option for very heavy dark matter masses.

13.2 Baryogenesis and Dark Matter from PBH evaporation and PBH relics

Here we discuss the possibility that evaporation stops at a mass $fM_{\rm Pl}$, leaving the dark matter produced by the PBH evaporation *together* with a second population of stable Planck-scale relics of mass $M_{\rm relic} = f \times M_{\rm Pl}$; we explore this two-component dark matter scenario on the same parameter space as before, taking into consideration the over-closure constraint from the PBH relics (the corresponding excluded region of parameter space is shaded in dark red, and is at the top left of the plots).

In the top four panels of fig. 13.2 we show the case where $f = 10^{-7}$. This is,

admittedly, a very low mass scale for PBH evaporation relics, but given ignorance about how evaporation might stop due to quantum gravity effects, it cannot be *a priori* ruled out. For such light PBH relics, we find that successful baryogenesis (via leptogenesis) plus two-component dark matter is possible for masses between roughly 10 MeV and a few GeV in the regime where $m_\chi < T_H$, and is possible again for very heavy dark matter $m_\chi > 10^{13}$ GeV (in the figure, we show $m_\chi = 10^{14}$ GeV), but in this case the contribution of Planck relics is very sub-dominant. The right-handed neutrino mass needs to be between 10^7 and 10^{12} GeV, and the PBH mass between 1 g and around a ton for this scenario to be successful in the low-dark matter mass regime; the heavy dark matter, as before, demand low right-handed neutrino masses, around 10^6 GeV or so. For dark matter larger than or around 10 GeV but lighter than around 10^{13} GeV, dark matter and the baryon asymmetry cannot be jointly produced; also, we find that GUT baryogenesis never works if Planck relics are around (the corresponding region of parameter space is ruled out by overclosure from the density of Planck relics, unless $f \to 0$).

The lower four panels show the case where evaporation stops *at the Planck scale*, i.e. $f = 1$. In this case the two-component dark matter is viable for a broad range of masses; demanding successful baryogenesis via leptogenesis forces the dark matter mass to be at the GeV scale (top left panel) and right handed neutrinos to be around 10 TeV; lighter dark matter particles in the MeV range are ruled out for $f \sim 1$, as are heavier masses (see top left panel showing $m_\chi = 100$ GeV). The bottom, left panel, with $m_\chi = 10^{13}$ GeV, shows (at around $M_{\rm PBH} \sim 1$ g) the turnover of the regime

when $m_\chi \sim T_H$; we do not find, however, regions of successful baryogenesis and dark matter; slightly heavier dark matter masses again make it possible to have successful leptogenesis, for sufficiently low right-handed neutrino masses (see bottom right panel, with $m_\chi = 10^{16}$ GeV).

13.2.1 Asymmetric Baryogenesis and Dark Matter from PBH evaporation

In the asymmetric dark matter scenario, in addition to the plots' parameter space, i.e. the $(M_{\rm PBH}, \beta)$ plane, the framework we consider has four additional parameters: the CP-asymmetry-washout-factor products $\epsilon_\chi \eta_\chi$ and $\epsilon_L \eta_L$, the dark matter mass m_χ, and the right-handed neutrino mass M_ν. We consider two representative right-handed neutrino mass scales, $M_\nu = 10^{11}$ GeV in fig. 13.3 and $M_\nu = 10^{13}$ GeV in fig. 13.4. In each of the top-four panels of each figure we fix the dark matter mass m_χ and show, on the $(M_{\rm PBH}, \beta)$ plane the necessary values for $\epsilon_\chi \eta_\chi$ to reproduce the universe's observed dark matter abundance, superimposed with regions where the baryon asymmetry can be produced for a given range of $\epsilon_L \eta_L$. Specifically, for definiteness we shade in light green the region corresponding to

$$10^{-8} < \epsilon_L \eta_L < 10^{-2}. \tag{13.1}$$

(Notice that a broader range is theoretically possible). For a given dark matter mass, we find that there is ample parameter space to produce the observed dark matter density via PBH evaporation and subsequent asymmetric right-handed neutrino decay. Of course,

from Eq. (12.41) it follows that the lower the dark matter mass, the larger the needed $\epsilon_\chi \eta_\chi$.

In fig. 13.3, the right-handed neutrino mass scale is low enough that for the relevant PBH mass range both $T_H > M_\nu$ and $T_H < M_\nu$ are possible (the latter at masses larger than around 100 grams, the former for lighter masses), hence the shape of the green-shaded regions. The figure illustrates that a broad range of dark matter masses are possible, depending on model details fixing the $\epsilon_\chi \eta_\chi$ and $\epsilon_L \eta_L$ products.

In the bottom four panels, we fix the product $\epsilon_\chi \eta_\chi$ to several different values, namely 10^{-6}, 10^{-5}, 10^{-4}, 10^{-3}, and show lines corresponding to values of the dark matter mass that, in turn, would produce the observed dark matter density. Again, a wide range of values for the dark matter mass is possible, depending on the value of the parameter $\epsilon_\chi \eta_\chi$. The lower $\epsilon_\chi \eta_\chi$, the heavier the possible range of masses where the asymmetric dark matter and baryon asymmetry generation is possible.

We note that the limits on the current dark matter velocity are here different than before. First, the dark matter originates from right-handed neutrino decays rather than directly from evaporation. The right-handed neutrino lifetime is always much shorter than the PBH evaporation time scale; hence, effectively, the right-handed neutrino has no time to redshift, and the dark matter is produced by immediate subsequent decay. Assuming for simplicity isotropic decays in the rest frame of the neutrino, as we show in the Appendix the average dark matter velocity in this case is a factor 2 smaller than in the case of direct production from evaporation. As a result, the constraints on the dark matter mass are generically a factor 2 weaker (see Appendix **??**).

However, since in the asymmetric dark matter production scenario we posit that processes exist that deplete the symmetric $\bar{\chi}\chi$ component produced by evaporation, the dark matter velocity might, and will, be affected by such processes. For instance, should the depletion of the symmetric component proceed via annihilation with the visible sector, i.e. $\bar{\chi}\chi \to$ SM, then the dark matter would be presumably brought in kinetic equilibrium and thus *cool* to the visible sector temperature, weakening the limit discussed above; if, on the other hand, the depletion occurs via $2n \to 2$ "cannibal" processes, with $n > 1$, such as $\bar{\chi}\chi\bar{\chi}\chi \to \bar{\chi}\chi$, then effectively the dark matter would *heat* itself up, strengthening the limits discussed above.

For reference, in the figures we leave a vertical thick blue line in the top-left panel, corresponding to the heating from sterile neutrino decay, with the understanding that such limits are model-dependent and could be stronger or weaker than what the lines indicates. In practice, however, these constraints are largely outside the region of parameter space of interest.

Notice that a similar discussion to what we treat in the Appendix would be in order if the dark sector particles contained particles with masses largely different from the dark matter mass they eventually decay into. As mentioned above, here we make the simplifying assumption that the dark sector spectrum is trivially degenerate at a mass scale close to m_χ.

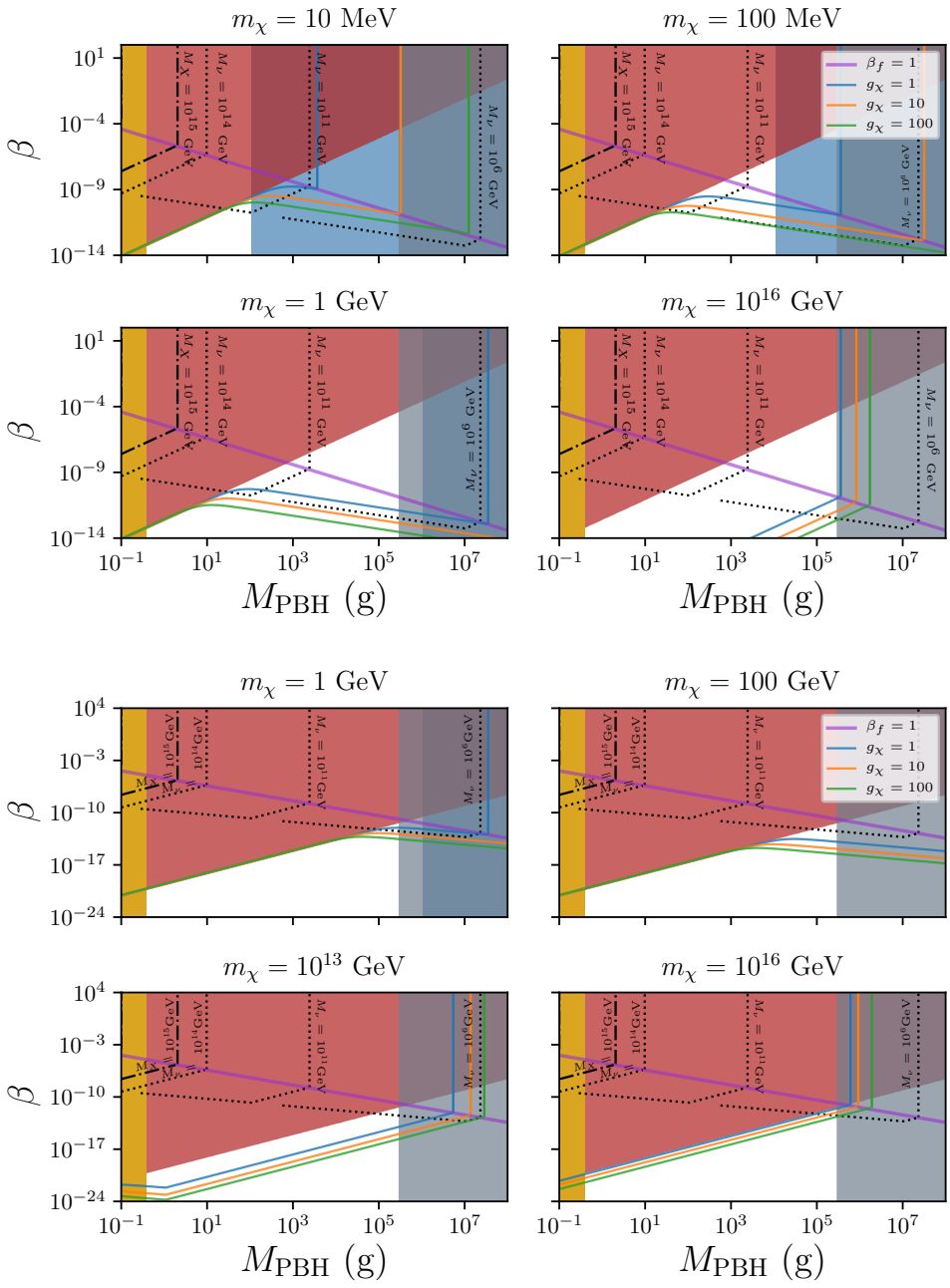

Figure 13.2: Top: Mixed-dark matter case, with Planck-scale relic of mass $M = fM_{\rm Pl}$, and $f = 10^{-7}$. The shaded region in the upper left indicates an excessive density of Planck-scale relics, all other lines are the same as in fig. 13.1. Bottom: same, for $f = 1$ (notice the different y axis).

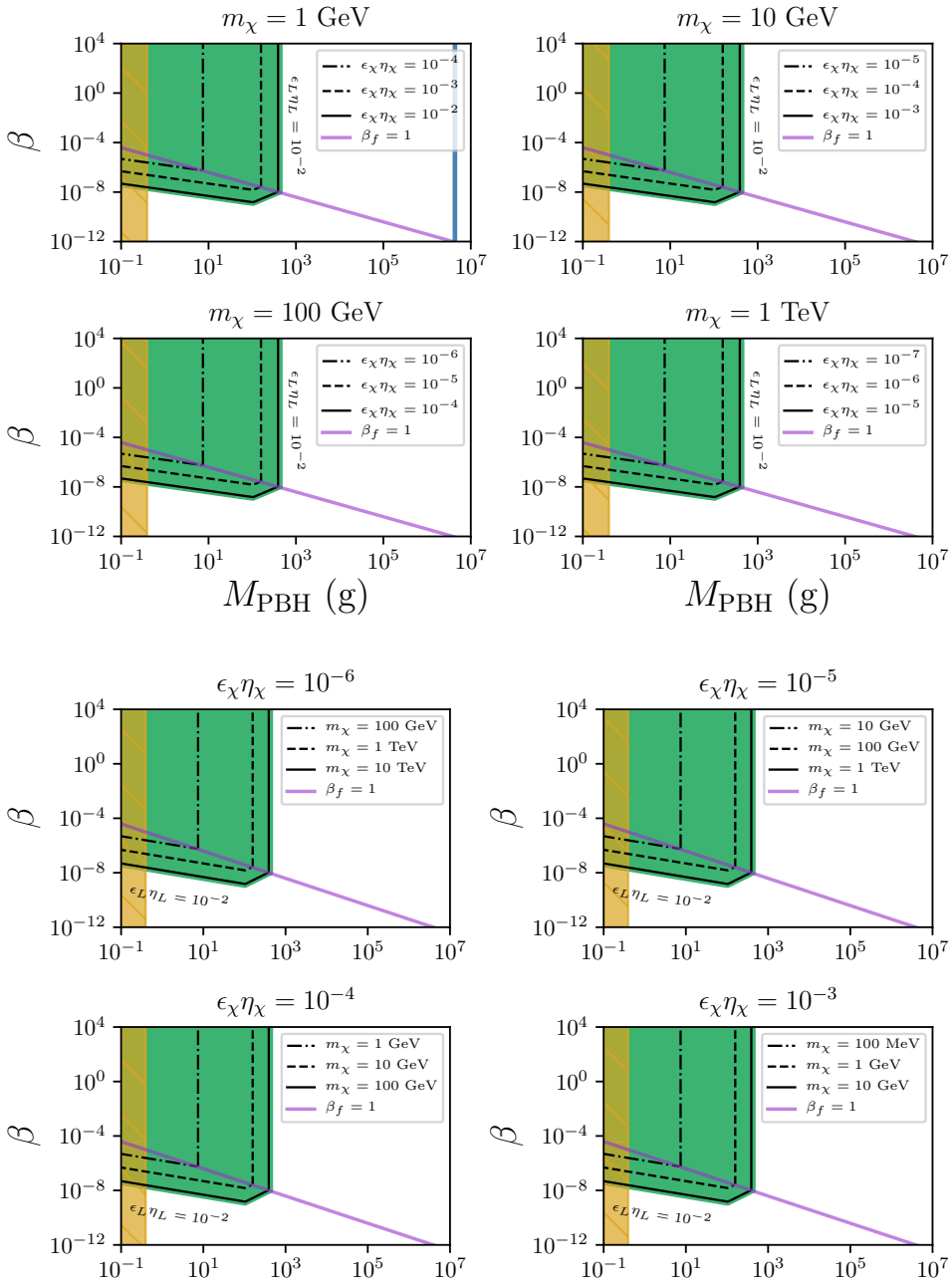

Figure 13.3: The Asymmetric Dark matter scenario, with $M_\nu = 10^{11}$ GeV. The green shaded region allows for successful asymmetric baryogenesis-via-leptogenesis, for $10^{-8} < \epsilon_L\eta_L < 10^{-2}$. Each panel in the top four plots assumes a different dark matter, mass, $m_\chi = 1$ GeV, 10 GeV, 100 GeV and 1 TeV. The black lines in those plots show the required values of $\epsilon_\chi\eta_\chi$ to produce the observed density of (asymmetric) dark matter. In the lower four panels, we instead fix $\epsilon_\chi\eta_\chi$ to several different values, 10^{-6}, 10^{-5}, 10^{-4}, 10^{-3}, and show lines corresponding to values of the dark matter mass that, in turn, would produce the observed dark matter density. As before, the purple line indicates $\beta_f = 1$. The vertical dark blue line shows the limit from the dark matter velocity.

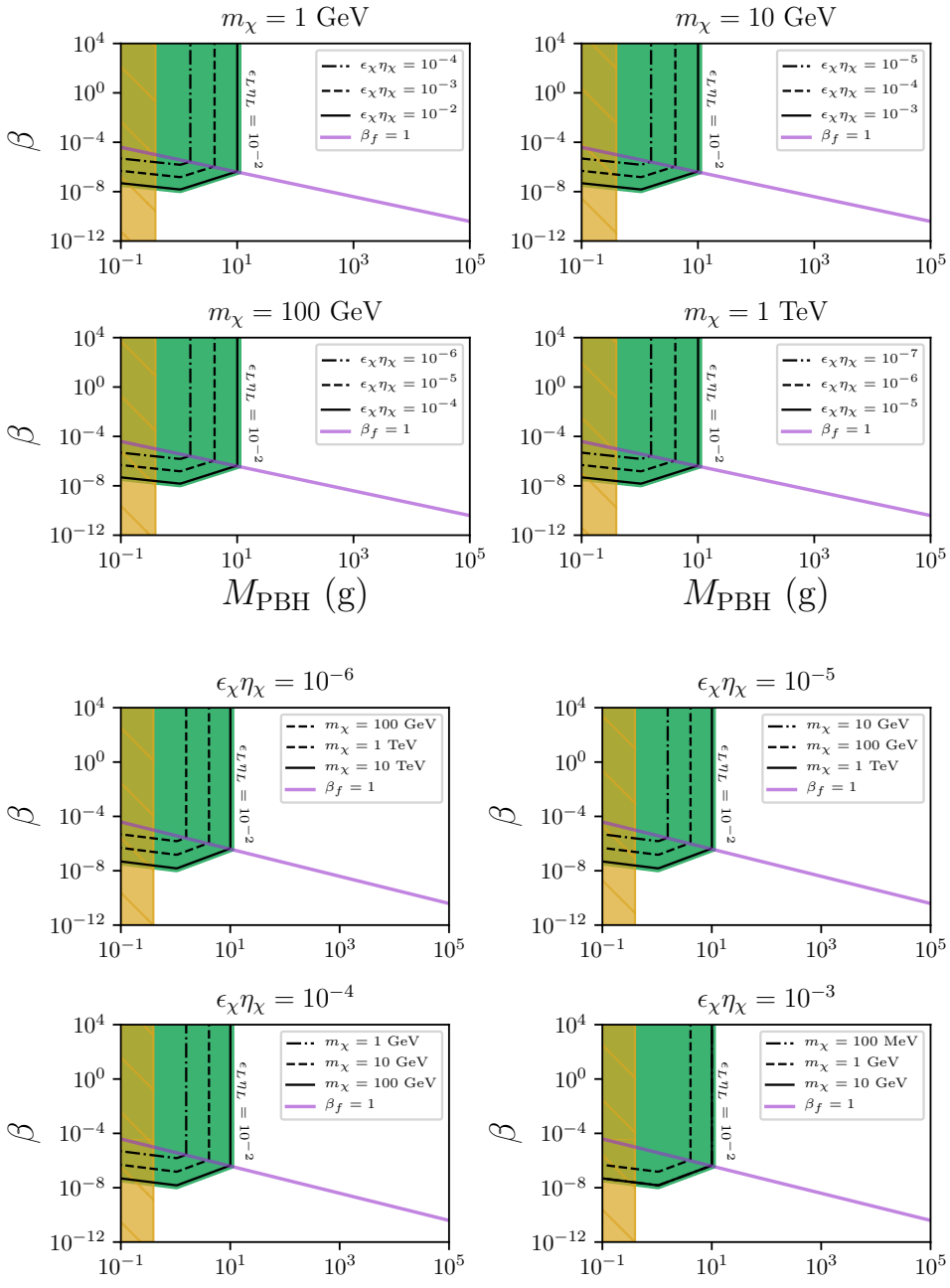

Figure 13.4: As in fig. 13.3, but with $M_\nu = 10^{13}$ GeV

Chapter 14

Discussion and Conclusions

We studied the joint production of the observed matter-antimatter asymmetry and of the cosmological dark matter from the evaporation of light primordial black holes (PBH) in the very early universe, at times $t_{\rm evap} \ll 1$ sec. The parameters of the model we considered include a universal mass for the primordial black holes, and their relative abundance at generation. We assumed that the dark matter belongs to a "dark sector" with a certain number of dark degrees of freedom. We also considered a "mixed dark matter scenario", where the dark matter is both produced by PBH evaporation and consists of PBH relics from the end of evaporation at around, or below, the Planck scale. Finally, we considered three scenarios for the generation of the matter-antimatter asymmetry: (i) CP- and B-violating decays of GUT gauge bosons, (ii) baryogenesis through (non-thermal) leptogenesis via out-of-equilibrium CP- and L- violating decays of heavy right-handed neutrinos, and (iii) asymmetric dark matter and baryogenesis, again via decays of heavy right handed neutrinos.

The parameter space under consideration is constrained by a variety of considerations, from limits on the dark matter velocity inherited from the large Hawking-Gibbons temperature scales at which the dark matter was produced, to limits on the PBH mass from the Hubble rate during inflation, to an excessive density of relic PBH from the end of evaporation at the Planck scale.

Unlike in previous studies that focused on scenarios where PBH dominate the energy density of the universe at production (see e.g. Ref. [52, 53]), here PBH can be a subdominant component to the early universe's energy density, with generally different conclusions (although our results correspond to those of Ref. [53] for values of β such that prior to evaporation PBH dominate the energy density of the universe).

If evaporation does not stop, and PBH vanish completely, both GUT baryogenesis and leptogenesis can be successful in conjunction with dark matter production from evaporation. GUT baryogenesis only works if the dark matter is between 1 and 10 MeV, while leptogenesis works either for dark matter masses between 1 MeV and a few GeV, or for super-heavy masses from 10^{13} to 10^{18} GeV, the maximal possible dark matter in this scenario. The needed PBH masses range from a few grams (for light dark matter particle masses), to around a ton for super-heavy dark matter.

If PBH evaporation does stop at some scale $fM_{\rm Pl}$, GUT baryogenesis is ruled out entirely, and leptogenesis works only for masses up to a few GeV or, again, for very heavy dark matter masses. In the former case, right handed neutrino masses must be large (10^{11} GeV or so), in the latter, they must be much lighter (10^{6} GeV or less).

Asymmetric dark matter and baryogenesis is successful, in this framework, for

a broad range of effective CP times washout factors $\epsilon\eta$ for the visible and dark sector. The larger the dark sector value of the product $\epsilon_\chi \eta_\chi$, the lighter the viable range of dark matter masses. The dark matter, in this scenario, must have a mass between a fraction of a GeV and 10 TeV or so.

If the scenario discussed here is indeed the backdrop for the generation of visible and dark matter, the detection outlook is relatively daunting. Searches for relic Planck-scale objects are possible, and in some cases might set some limits on this scenario, especially if the relic PBH are a substantial fraction of the dark matter, and/or if the relic are charged [77]. Directly or indirectly detecting the dark matter produced in PBH evaporation in the present scenario is problematic: since we assume no thermal equilibrium at any temperature, the indirect detection rates generically are highly suppressed, and so are the direct detection rates.

One possible route to test this scenario (and in fact any scenario involving light PBH) is to look for gravitational wave emission from evaporation [78]: while all evaporation products quickly thermalize in our scenario, gravitons do not, leaving an imprint that is in principle detectable. There is a one-to-one correspondence between the frequency ν of gravity waves at the present time and the corresponding frequency at emission ν_*, emission which assume here to happen at the PBH evaporation time:

$$\nu \simeq 0.34\ \nu_*\ \frac{T_0}{T_*} \left(\frac{100}{g_*(T_{\rm evap})} \right)^{1/3}, \tag{14.1}$$

where the temperature of the PBH evaporation $T_{\rm evap}$ is given in Eq. (11.8) and T_0

corresponds to the CMB frequency, around 160.4 GHz. As a result, we have

$$\nu \simeq 7.1 \times 10^{10}\ \text{Hz} \left(\frac{\nu_*}{M_{\rm Pl}}\right) \left(\frac{100}{g_*(T_{\rm evap})}\right)^{1/12} \left(\frac{g}{100}\right)^{-1/2} \left(\frac{M_{\rm PBH}}{M_{\rm Pl}}\right)^{3/2}. \tag{14.2}$$

The maximal value for ν_* is around a few times the Hawking-Gibbons temperature, $T_H = M_{\rm Pl}^2/M_{\rm PBH}$. Using Eq. (14.1), we get that the maximal frequency of gravity waves today is around 10^{16} Hz. Generally, the spectrum peaks at $\nu_* \sim 2.8 T_H$ [78], therefore producing a signal at frequencies much higher than current gravity wave detectors. As we explain below, detection is however possible through the inverse Gertsenshtein effect [79, 80].

We estimate here the strain corresponding to the predicted gravity wave signal from PBH evaporation. Ref. [78] calculates that the energy density of gravity waves from PBH evaporation integrated over frequencies, and accounting for our assumption that PBH do not dominate the energy density of the universe, but rather constitute a fraction β of it at production, is approximately

$$\Omega_{\rm GW}(t_{\rm evap}) \simeq 0.006 \left(\frac{g_G}{100}\right)^2 \beta, \tag{14.3}$$

with $g_G = 2$ the number of graviton degrees of freedom. The equation above also assumes graviton production to happen instantaneously at the evaporation time (see also Ref. [53]). The red-shifted gravitational wave density today is

$$\Omega_{\rm GW} h^2(t_{\rm now}) \simeq 1.67 \times 10^{-5} \left(\frac{100}{g_*(T_{\rm evap})}\right)^{1/3} \Omega_{\rm GW}(t_{\rm evap}) \simeq 10^{-11} \left(\frac{g_G}{10^{-2}}\right)^2 \beta. \tag{14.4}$$

The corresponding strain is then

$$h \sim 10^{-36} \beta^{1/2}. \tag{14.5}$$

The frequencies for the gravity wave emitted from PBH evaporation are well beyond currently operating or future interferometers; however they could be detectable via the so-called inverse Gertsenshtein effect [81]: The passage of gravity waves in a static magnetic field sources electromagnetic waves. As long as the induced signal "beats" thermal noise, a signal can be detected [79, 80].

In conclusion, early evaporation of light primordial black holes can lead to co-genesis of a baryon asymmetry and of the dark matter. We demonstrated that several possible baryogenesis scenarios are viable (GUT baryogenesis, leptogenesis, asymmetric dark matter), for a broad range of dark matter masses and of primordial black hole masses. The dark matter itself can originate entirely from evaporation, or from decay of particles produced by PBH evaporation, or it can be a mix of particles from evaporation, and Planck-scale relics of the evaporation process. Detection prospects for the dark matter are discouraging, but this scenario would leave an imprint of very high-frequency gravitational waves, of calculable spectrum and intensity, possibly detectable via the inverse Gertsenshtein effect.

Bibliography

[1] S. Perlmutter et al. Measurements of Omega and Lambda from 42 high redshift supernovae. *Astrophys. J.*, 517:565–586, 1999.

[2] N. Aghanim et al. Planck 2018 results. VI. Cosmological parameters. 7 2018.

[3] Will J. Percival et al. Baryon Acoustic Oscillations in the Sloan Digital Sky Survey Data Release 7 Galaxy Sample. *Mon. Not. Roy. Astron. Soc.*, 401:2148–2168, 2010.

[4] Steven Weinberg. The Cosmological Constant Problem. *Rev. Mod. Phys.*, 61:1–23, 1989. [,569(1988)].

[5] Raphael Bousso and Joseph Polchinski. Quantization of four form fluxes and dynamical neutralization of the cosmological constant. *JHEP*, 06:006, 2000.

[6] Shamit Kachru, Renata Kallosh, Andrei D. Linde, and Sandip P. Trivedi. De Sitter vacua in string theory. *Phys. Rev.*, D68:046005, 2003.

[7] Michael Dine and Nathan Seiberg. Is the Superstring Weakly Coupled? *Phys. Lett.*, 162B:299–302, 1985.

[8] Georges Obied, Hirosi Ooguri, Lev Spodyneiko, and Cumrun Vafa. De Sitter Space and the Swampland. 2018.

[9] David Andriot. On the de Sitter swampland criterion. *Phys. Lett.*, B785:570–573, 2018.

[10] David Andriot and Christoph Roupec. Further refining the de Sitter swampland conjecture. *Fortsch. Phys.*, 67(1-2):1800105, 2019.

[11] Daniel Junghans. Weakly Coupled de Sitter Vacua with Fluxes and the Swampland. *JHEP*, 03:150, 2019.

[12] Niccolò Cribiori and Daniel Junghans. No classical (anti-)de Sitter solutions with O8-planes. *Phys. Lett. B*, 793:54–58, 2019.

[13] Andreas Banlaki, Abhishek Chowdhury, Christoph Roupec, and Timm Wrase. Scaling limits of dS vacua and the swampland. *JHEP*, 03:065, 2019.

[14] Savdeep Sethi. Supersymmetry Breaking by Fluxes. *JHEP*, 10:022, 2018.

[15] Thomas W. Grimm, Chongchuo Li, and Irene Valenzuela. Asymptotic Flux Compactifications and the Swampland. *JHEP*, 06:009, 2020.

[16] Sumit K. Garg and Chethan Krishnan. Bounds on Slow Roll and the de Sitter Swampland. *JHEP*, 11:075, 2019.

[17] Sumit K. Garg, Chethan Krishnan, and M. Zaid Zaz. Bounds on Slow Roll at the Boundary of the Landscape. *JHEP*, 03:029, 2019.

[18] Jonathan J. Heckman, Craig Lawrie, Ling Lin, and Gianluca Zoccarato. F-theory and Dark Energy. *Fortsch. Phys.*, 67(10):1900057, 2019.

[19] Jonathan J. Heckman, Craig Lawrie, Ling Lin, Jeremy Sakstein, and Gianluca Zoccarato. Pixelated Dark Energy. *Fortsch. Phys.*, 67(11):1900071, 2019.

[20] Hao Geng. A Potential Mechanism for Inflation from Swampland Conjectures. *Phys. Lett. B*, 805:135430, 2020.

[21] John March-Russell and Rudin Petrossian-Byrne. QCD, Flavor, and the de Sitter Swampland. 6 2020.

[22] Michele Cicoli, Senarath De Alwis, Anshuman Maharana, Francesco Muia, and Fernando Quevedo. De Sitter vs Quintessence in String Theory. *Fortsch. Phys.*, 67(1-2):1800079, 2019.

[23] Michele Cicoli, Fernando Quevedo, and Roberto Valandro. De Sitter from T-branes. *JHEP*, 03:141, 2016.

[24] Michele Cicoli, Denis Klevers, Sven Krippendorf, Christoph Mayrhofer, Fernando Quevedo, and Roberto Valandro. Explicit de Sitter Flux Vacua for Global String Models with Chiral Matter. *JHEP*, 05:001, 2014.

[25] Michele Cicoli, Anshuman Maharana, F. Quevedo, and C.P. Burgess. De Sitter String Vacua from Dilaton-dependent Non-perturbative Effects. *JHEP*, 06:011, 2012.

[26] Donald Marolf, Ian A. Morrison, and Mark Srednicki. Perturbative S-matrix for massive scalar fields in global de Sitter space. *Class. Quant. Grav.*, 30:155023, 2013.

[27] David Andriot, Paul Marconnet, and Timm Wrase. New de Sitter solutions of 10d type IIB supergravity. 5 2020.

[28] David Andriot, Paul Marconnet, and Timm Wrase. Intricacies of classical de Sitter string backgrounds. 6 2020.

[29] Tom Banks and Michael Dine. Dark energy in perturbative string cosmology. *JHEP*, 10:012, 2001.

[30] Sidney R. Coleman and Frank De Luccia. Gravitational Effects on and of Vacuum Decay. *Phys. Rev.*, D21:3305, 1980.

[31] Sidney R. Coleman. The Fate of the False Vacuum. 1. Semiclassical Theory. *Phys. Rev.*, D15:2929–2936, 1977. [Erratum: Phys. Rev.D16,1248(1977)].

[32] Hirosi Ooguri, Eran Palti, Gary Shiu, and Cumrun Vafa. Distance and de Sitter Conjectures on the Swampland. *Phys. Lett.*, B788:180–184, 2019.

[33] Shamit Kachru, Manki Kim, Liam McAllister, and Max Zimet. de Sitter Vacua from Ten Dimensions. 2019.

[34] Michael Dine, Guido Festuccia, and Alexander Morisse. The Fate of Nearly Supersymmetric Vacua. *JHEP*, 09:013, 2009.

[35] Alek Bedroya and Cumrun Vafa. Trans-Planckian Censorship and the Swampland. *JHEP*, 09:123, 2020.

[36] Michael Dine, Jamie A. P. Law-Smith, Shijun Sun, Duncan Wood, and Yan Yu. Obstacles to Constructing de Sitter Space in String Theory. *JHEP*, 02:050, 2021.

[37] Shinji Tsujikawa. Quintessence: A Review. *Class. Quant. Grav.*, 30:214003, 2013.

[38] Michael Dine, Guido Festuccia, and Alexander Morisse. The Fate of Nearly Supersymmetric Vacua. *JHEP*, 09:013, 2009.

[39] Stefano Profumo. *An Introduction to Particle Dark Matter*. World Scientific, 2017.

[40] Csaba Balazs. Baryogenesis: A small review of the big picture. 2014.

[41] B. P. Abbott et al. Observation of Gravitational Waves from a Binary Black Hole Merger. *Phys. Rev. Lett.*, 116(6):061102, 2016.

[42] Simeon Bird, Ilias Cholis, Julian B. Muñoz, Yacine Ali-Haïmoud, Marc Kamionkowski, Ely D. Kovetz, Alvise Raccanelli, and Adam G. Riess. Did LIGO detect dark matter? *Phys. Rev. Lett.*, 116(20):201301, 2016.

[43] Yuta Hamada and Satoshi Iso. Baryon asymmetry from primordial black holes. *PTEP*, 2017(3):033B02, 2017.

[44] James M. Cline. TASI Lectures on Early Universe Cosmology: Inflation, Baryogenesis and Dark Matter. 2018.

[45] S. W. Hawking. Particle creation by black holes. *Communications in Mathematical Physics*, 43:199–220, August 1975.

[46] Y. B. Zel'dovich. Charge asymmetry of the universe as a consequence of evaporation of black holes and of the asymmetry of the weak interaction. *Soviet Journal of Experimental and Theoretical Physics Letters*, 24:25, July 1976.

[47] B. J. Carr. Some cosmological consequences of primordial black-hole evaporations. *Astroph. J.*, 206:8–25, May 1976.

[48] D. Toussaint, S. B. Treiman, Frank Wilczek, and A. Zee. Matter - Antimatter Accounting, Thermodynamics, and Black Hole Radiation. *Phys. Rev.*, D19:1036–1045, 1979.

[49] Michael S. Turner. BARYON PRODUCTION BY PRIMORDIAL BLACK HOLES. *Phys. Lett.*, 89B:155–159, 1979.

[50] A. F. Grillo. Primordial Black Holes and Baryon Production in Grand Unified Theories. *Phys. Lett.*, 94B:364–366, 1980.

[51] S. W. Hawking, I. G. Moss, and J. M. Stewart. Bubble Collisions in the Very Early Universe. *Phys. Rev.*, D26:2681, 1982.

[52] Daniel Baumann, Paul J. Steinhardt, and Neil Turok. Primordial Black Hole Baryogenesis. 2007.

[53] Tomohiro Fujita, Masahiro Kawasaki, Keisuke Harigaya, and Ryo Matsuda. Baryon

asymmetry, dark matter, and density perturbation from primordial black holes. *Phys. Rev.*, D89(10):103501, 2014.

[54] Olivier Lennon, John March-Russell, Rudin Petrossian-Byrne, and Hannah Tillim. Black Hole Genesis of Dark Matter. *JCAP*, 1804(04):009, 2018.

[55] Rouzbeh Allahverdi, James Dent, and Jacek Osinski. Nonthermal production of dark matter from primordial black holes. *Phys. Rev.*, D97(5):055013, 2018.

[56] Nicole F. Bell and R. R. Volkas. Mirror matter and primordial black holes. *Phys. Rev.*, D59:107301, 1999.

[57] Anson Hook. Baryogenesis from Hawking Radiation. *Phys. Rev.*, D90(8):083535, 2014.

[58] Y. B. Zel'dovich and I. D. Novikov. The Hypothesis of Cores Retarded during Expansion and the Hot Cosmological Model. *Astronomicheskii Zhurnal*, 43:758, 1966.

[59] Lawrence J. Hall, Karsten Jedamzik, John March-Russell, and Stephen M. West. Freeze-In Production of FIMP Dark Matter. *JHEP*, 03:080, 2010.

[60] Bernard J. Carr, J. H. Gilbert, and James E. Lidsey. Black hole relics and inflation: Limits on blue perturbation spectra. *Phys. Rev.*, D50:4853–4867, 1994.

[61] D. K. Nadezhin, I. D. Novikov, and A. G. Polnarev. Hydrodynamics of primordial black hole formation. *Astronomicheskii Zhurnal*, 55:216–230, April 1978.

[62] Benjamin V. Lehmann, Stefano Profumo, and Jackson Yant. The Maximal-Density Mass Function for Primordial Black Hole Dark Matter. *JCAP*, 1804(04):007, 2018.

[63] Y. Akrami et al. Planck 2018 results. X. Constraints on inflation. 2018.

[64] B. J. Carr, Kazunori Kohri, Yuuiti Sendouda, and Jun'ichi Yokoyama. New cosmological constraints on primordial black holes. *Phys. Rev.*, D81:104019, 2010.

[65] Don N. Page. Particle Emission Rates from a Black Hole: Massless Particles from an Uncharged, Nonrotating Hole. *Phys. Rev.*, D13:198–206, 1976.

[66] Don N. Page. Particle Emission Rates from a Black Hole. 2. Massless Particles from a Rotating Hole. *Phys. Rev.*, D14:3260–3273, 1976.

[67] Don N. Page. Particle Emission Rates from a Black Hole. 3. Charged Leptons from a Nonrotating Hole. *Phys. Rev.*, D16:2402–2411, 1977.

[68] N. Aghanim et al. Planck 2018 results. VI. Cosmological parameters. 2018.

[69] Matteo Viel, Julien Lesgourgues, Martin G. Haehnelt, Sabino Matarrese, and Antonio Riotto. Constraining warm dark matter candidates including sterile neutrinos and light gravitinos with WMAP and the Lyman-alpha forest. *Phys. Rev.*, D71:063534, 2005.

[70] Marion Flanz, Emmanuel A. Paschos, Utpal Sarkar, and Jan Weiss. Baryogenesis through mixing of heavy Majorana neutrinos. *Phys. Lett.*, B389:693–699, 1996.

[71] Apostolos Pilaftsis. CP violation and baryogenesis due to heavy Majorana neutrinos. *Phys. Rev.*, D56:5431–5451, 1997.

[72] W. Buchmuller, P. Di Bari, and M. Plumacher. Cosmic microwave background, matter - antimatter asymmetry and neutrino masses. *Nucl. Phys.*, B643:367–390, 2002. [Erratum: Nucl. Phys.B793,362(2008)].

[73] Lawrence J. Hall, Yasunori Nomura, and Satoshi Shirai. Grand Unification, Axion, and Inflation in Intermediate Scale Supersymmetry. *JHEP*, 06:137, 2014.

[74] M. Fukugita and T. Yanagida. Resurrection of grand unified theory baryogenesis. *Phys. Rev. Lett.*, 89:131602, 2002.

[75] Adam Falkowski, Joshua T. Ruderman, and Tomer Volansky. Asymmetric Dark Matter from Leptogenesis. *JHEP*, 05:106, 2011.

[76] Jeffrey A. Harvey and Michael S. Turner. Cosmological baryon and lepton number in the presence of electroweak fermion number violation. *Phys. Rev.*, D42:3344–3349, 1990.

[77] E. M. Drobyshevski, M. E. Drobyshevski, S. A. Ponyaev, and I. S. Guseva. Daemons: Detection at Pulkovo, Gran Sasso, and Soudan. *Mod. Phys. Lett.*, A27:1250085, 2012.

[78] Alexander D. Dolgov and Damian Ejlli. Relic gravitational waves from light primordial black holes. *Phys. Rev.*, D84:024028, 2011.

[79] A. M. Cruise. The potential for very high-frequency gravitational wave detection. *Class. Quant. Grav.*, 29:095003, 2012.

[80] Fangyu Li, Robert M. L. Baker, Jr., Zhenyun Fang, Gary V. Stephenson, and Zhenya Chen. Perturbative Photon Fluxes Generated by High-Frequency Gravitational Waves and Their Physical Effects. *Eur. Phys. J.*, C56:407–423, 2008.

[81] W. K. De Logi and A. R. Mickelson. Electrogravitational Conversion Cross-Sections in Static Electromagnetic Fields. *Phys. Rev.*, D16:2915–2927, 1977.

[82] Steven Weinberg. Anthropic Bound on the Cosmological Constant. *Phys. Rev. Lett.*, 59:2607, 1987.

[83] Alan H. Guth. The Inflationary Universe: A Possible Solution to the Horizon and Flatness Problems. *Adv. Ser. Astrophys. Cosmol.*, 3:139–148, 1987.

[84] Alexei A. Starobinsky. A New Type of Isotropic Cosmological Models Without Singularity. *Adv. Ser. Astrophys. Cosmol.*, 3:130–133, 1987.

[85] A.D. Linde. A new inflationary universe scenario: A possible solution of the horizon, flatness, homogeneity, isotropy and primordial monopole problems. *Physics Letters B*, 108(6):389 – 393, 1982.

[86] Andreas Albrecht and Paul J. Steinhardt. Cosmology for Grand Unified Theories with Radiatively Induced Symmetry Breaking. *Adv. Ser. Astrophys. Cosmol.*, 3:158–161, 1987.

[87] Planck 2018 results. vi. cosmological parameters, 2018.

[88] Martin Lemoine. Moduli constraints on primordial black holes. *Phys. Lett.*, B481:333–338, 2000.

[89] I. B. Zeldovich and A. A. Starobinskii. Possibility of a cold cosmological singularity in the spectrum of primordial black holes. *ZhETF Pisma Redaktsiiu*, 24:616–618, December 1976.

[90] Stephen Hawking. Gravitationally collapsed objects of very low mass. *Mon. Not. Roy. Astron. Soc.*, 152:75, 1971.

[91] Tomohiro Nakama, Tomohiro Harada, A. G. Polnarev, and Jun'ichi Yokoyama. Identifying the most crucial parameters of the initial curvature profile for primordial black hole formation. *JCAP*, 1401:037, 2014.

[92] Tomohiro Harada, Chul-Moon Yoo, and Kazunori Kohri. Threshold of primordial black hole formation. *Phys. Rev.*, D88(8):084051, 2013. [Erratum: Phys. Rev.D89,no.2,029903(2014)].

[93] Ilia Musco and John C. Miller. Primordial black hole formation in the early universe: critical behaviour and self-similarity. *Class. Quant. Grav.*, 30:145009, 2013.

[94] Masaru Shibata and Misao Sasaki. Black hole formation in the Friedmann universe: Formulation and computation in numerical relativity. *Phys. Rev.*, D60:084002, 1999.